Master Thesis 112

Data-Driven Controller Design via Finite-Horizon Dissipativity

Master Thesis

Nils Wieler

March 31, 2021

PrüferIn: *Prof. Dr. Frank Allgöwer*
BetreuerIn: *Julian Berberich, M.Sc.*
Anne Koch, M.Sc.

Institut für Systemtheorie und Regelungstechnik
Universität Stuttgart
Prof. Dr.-Ing. Frank Allgöwer

Abstract

In this thesis, a framework for data-driven controller design for single-input single-output (SISO) plants in the standard feedback loop based on closed-loop finite-horizon dissipativity is presented. The work builds upon existing literature in the data-driven setting for parametrizing trajectories of an open-loop linear time-invariant (LTI) system and performing a finite-horizon dissipativity analysis on an open-loop system. These works are naturally extended in the way that, first, all closed-loop trajectories of the standard feedback loop are parametrized using given input-output data of the plant and a model of the controller. Secondly, the newly gained parametrization of closed-loop trajectories is used for simulation in the standard feedback loop and for developing necessary and sufficient conditions for closed-loop finite-horizon dissipativity in terms of a definiteness condition on a single matrix. Thereafter, for controller synthesis with desired closed-loop dissipativity specifications, the definiteness conditions are turned into a quadratic matrix inequality feasibility problem (QMIFP) in the controller parameters. Hence, a purely data-driven synthesis inequality leading to a desired closed-loop dissipativity property is obtained. The resulting controller design method allows to perform multiobjective structured controller synthesis. Finally, methods for solving the synthesis quadratic matrix inequality (QMI) are presented for both the convex and non-convex case, which are used in a concluding simulation example, where the results of this thesis are applied.

Contents

List of abbreviations

ILC	Iterative Learning Control
VRFT	Virtual Reference Feedback Tuning
LMI	linear matrix inequality
QMI	quadratic matrix inequality
QMIFP	quadratic matrix inequality feasibility problem
DC	difference of convex functions
DCA	difference of convex functions algorithm
SISO	single-input single-output
MIMO	multiple-input multiple-output
LTI	linear time-invariant
DT	discrete-time

Notation

$\mathbb{R}$	Set of real numbers.
$\mathbb{S}^n$	Set of real symmetric matrices of dimension $n \times n$.
$\lvert x \rvert$	Absolute value of $x \in \mathbb{R}$.
$\lVert x \rVert_2$	l_2-norm of $x \in \mathbb{R}^n$.
I_n	Identity matrix of dimension $n \times n$.
$0_{n \times m}$	Zero matrix of dimension $n \times m$.
0_n	Zero matrix of dimension $n \times n$.
$A^\top$	Transpose of the matrix $A \in \mathbb{R}^{n \times m}$.
A^{-1}	Inverse of the matrix $A \in \mathbb{R}^{n \times n}$.
$A^\perp$	Basis matrix of the kernel of the matrix $A \in \mathbb{R}^{n \times m}$.
$A \succ 0$ $(A \succcurlyeq 0)$	Matrix $A \in \mathbb{S}^n$ and is positive (semi)definite.
$A \prec 0$ $(A \preccurlyeq 0)$	Matrix $A \in \mathbb{S}^n$ and is negative (semi)definite.
$\mathrm{col}(A)$	Column space of the matrix $A \in \mathbb{R}^{n \times m}$.
$\mathrm{rank}(A)$	Rank of the matrix $A \in \mathbb{R}^{n \times m}$.
$\mathrm{trace}(A)$	Trace of the matrix $A \in \mathbb{R}^{n \times n}$.
$\otimes$	Kronecker product.
$\dim(\mathbb{V})$	Dimension of the vector space $\mathbb{V}$.
$\langle \cdot, \cdot \rangle$	Inner product $\langle \cdot, \cdot \rangle : \mathbb{V} \times \mathbb{V} \mapsto \mathbb{R}$ of the vector space $\mathbb{V}$.
$f^* : \mathbb{R}^n \mapsto \mathbb{R} \cup \{\infty\}$	The conjugate of $f : \mathbb{R}^n \mapsto \mathbb{R}$ defined by $f^*(y) = \sup\{\langle x, y \rangle - f(x) : x \in \mathbb{R}^n\}$.
$\partial f(x)$	Subdifferential of f at x (set of all subgradients).

1. Introduction

1.1. Motivation

The majority of the results in control theory are based on the knowledge of a mathematical model of the system one wants to control. There are many different control approaches and methods available in the model-based theory. These methods are well established and successfully used in various practical applications and a number of different fields. For instance, the notion of dissipativity, introduced by Willems [36, 37], is one of the most important and widely used concepts in both theory and practice. Dissipativity is used for systems analysis as well as for controller design. In particular, the key underlying concept in controller design, e.g., $\mathcal{H}_\infty$-design or positive real design, is dissipativity. Performance criteria for the closed loop can be stated as dissipativity conditions and turned into tractable linear matrix inequalitys (LMIs) in the controller parameters [31].

The main drawback of model-based control is the necessity of a well-suited model for the true dynamics of the plant. Therefore, it is required to get quite accurate models from first principles or use techniques from robust control to handle the unmodeled dynamics via an uncertainty description. Both, deriving an accurate model or a good uncertainty description for the plant can be challenging. With the increasing complexity of systems, modeling a system by first principles becomes even more difficult. In addition, not only the complexity of systems is increasing, the available data from these systems is rising exponentially (see Figure 1.1) due to the ongoing digitalization. Because of that increase in data, system identification [20] and data-driven control methods have become more and more important. Via system identification one tries to identify a model from the data and use the existing model-based methods to control the system. Therefore, two steps are needed to design controllers, whereas the data-driven methods skip the modeling part and the given data is used directly for controller design and provide guarantees directly from the available data. For example, Iterative Learning Control (ILC) [7, 27] is a data-driven method for reference tracking, if a machine (e.g. robot) does the same task repeatedly. The

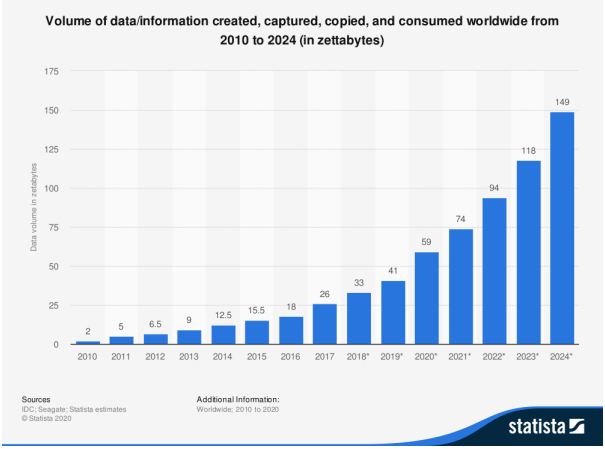

Figure 1.1.: Increasing amount of available data (see [15]).

control input for the next task-iteration is adapted based on the knowledge from prior iterations to reduce the tracking error. Therefore, no model is needed since the control input update is purely based on measurements of the last iterations. Another data-driven method is Virtual Reference Feedback Tuning (VRFT) [8], where the minimization of standard model-reference performance indices is performed via input-output measurements, i.e., finding a controller that minimizes a model-reference problem is solved only by using measurements of the plant. An introduction to data-driven control in general and a more complete summary over the existing methods is available in [14].

However, many of the developed data-driven methods lack the well-known guarantees for stability, performance, and robustness from the model-based setting. To overcome these issues, the so-called *Fundamental Lemma* by [38] has gained increasing attention in data-driven control, since it provides a powerful approach to replace the usual mathematical model with a representation of the system directly on the basis of data. It was successfully applied in several fields, for example in data-driven simulation [23], controller design (e.g. [4, 11, 22, 25]) and model predictive control [3, 9]. Further, in [16, 24, 29] it is used for a dissipativity analysis on an open-loop system.

1.2. Contribution and outline

The goal of this thesis is to formulate a controller design framework based on finite-horizon dissipativity for SISO LTI discrete-time (DT) systems in the standard feedback loop (see Figure 1.2) using only measured data of the plant.

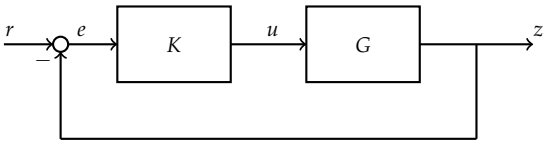

Figure 1.2.: Standard feedback loop.

Hence, this thesis contributes to the general dissipativity controller design methods in the data-driven setting. Since, from a practical point of view, the measured data of the plant can only contain input-ouput data and generally no state measurements, these dissipativity conditions have to be formulated in the input-output context.

Therefore, the work of [29] for the dissipativity analysis of an open-loop system is extended to perform analysis on the closed loop. To this end, a parametrization of all closed-loop trajectories in the standard feedback loop, based on given data of the plant and a model of the controller, employing Willems' *Fundamental Lemma*, is presented. This parametrization is then used for closed-loop data-driven simulation, similar to the simulation of an open-loop system in [23]. Furthermore, this developed representation of closed-loop trajectories is used to derive necessary and sufficient conditions for finite-horizon closed-loop dissipativity. Finally, it is shown how these conditions can be used for controller design. Therefore, the conditions are translated into a QMIFP in the controller parameters and then solved using a difference of convex functions (DC) programming method [18, 28].

The thesis is structured as follows. In Chapter 2, the theoretical foundations are introduced by explaining important definitions and existing results in the data-driven setting. Furthermore, Chapter 3 provides the closed-loop trajectory parametrization and the resulting necessary and sufficient conditions for closed-loop dissipativity. Next, in Chapter 4, the controller synthesis framework for closed-loop finite-horizon dissipativity in form of a

QMIFP and a demonstration on an example system is presented. Finally, the thesis is concluded in Chapter 5.

The results of this master thesis have also already been submitted and accepted for publication at the 3^{rd} *Annual Learning for Dynamics & Control Conference*. Hence, this thesis is based on and taken in parts literally from [35].

1.3. Notation

In this thesis, the following notation is used. For a finite sequence $\{x_k\}_{k=0}^{N-1}$, $x_k \in \mathbb{R}^n$, of length N, x is used to denote either the sequence itself or the stacked vector

$$\begin{pmatrix} x_0 \\ \vdots \\ x_{N-1} \end{pmatrix} \quad \in \mathbb{R}^{Nn}$$

containing the components of the sequence. For such a sequence x, the *Hankel* matrix of depth L is given by

$$H_L(x) = \begin{pmatrix} x_0 & x_1 & \cdots & x_{N-L} \\ x_1 & x_2 & \cdots & x_{N-L+1} \\ \vdots & \vdots & \ddots & \vdots \\ x_{L-1} & x_L & \cdots & x_{N-1} \end{pmatrix}$$

and for a one-dimensional sequence, with $n = 1$, the lower-triangular *Toeplitz* matrix is given by

$$T(x) = \begin{pmatrix} x_0 & 0 & \cdots & 0 \\ x_1 & x_0 & \ddots & \vdots \\ \vdots & \vdots & \ddots & 0 \\ x_{N-1} & x_{N-2} & \cdots & x_0 \end{pmatrix}.$$

A matrix inequality $Q(\xi) \preccurlyeq 0$ in $\xi \in \mathbb{R}^{n_q}$ is called QMI, if $Q(\xi)$ is quadratic in ξ, i.e., of the form

$$Q(\xi) = Q_0 + \sum_{i=1}^{n_q} \xi_i Q_i + \sum_{i=1}^{n_q} \sum_{j=1}^{n_q} \xi_i \xi_j Q_{ij}, \tag{1.1}$$

where Q_0, $Q_i \in \mathbb{S}$ for $i = 0,\ldots,n_q$ and $Q_{ij} \in \mathbb{S}$ for $i,j = 1,\ldots,n_q$ are symmetric matrices of the same dimension. For a set $\mathcal{C}$ the indicator function is defined as

$$i_{\mathcal{C}}(x) = \begin{cases} 0, & \text{for } x \in \mathcal{C} \\ \infty, & \text{for } x \notin \mathcal{C} \end{cases} .$$

The set $\mathcal{C}$ is convex if and only if its indicator function $i_{\mathcal{C}}$ is convex.

2. Data-driven control framework

This chapter describes the theoretical foundation for the data-driven setting in this thesis. First, in Section 2.1, the system representation via the *Fundamental Lemma*, using only measured data, is presented. Furthermore, this representation is used in Section 2.2 for a data-driven finite-horizon dissipativity characterization.

2.1. Trajectory-based representation of LTI systems

Throughout the whole thesis, LTI DT systems are considered, where an input-output trajectory of such system is given by following definition.

Definition 2.1 *An input-output sequence* $\{u_k,y_k\}_{k=0}^{N-1}$ *with* $u_k \in \mathbb{R}^m$, $y_k \in \mathbb{R}^p$ *is a trajectory of a DT LTI system G, if there exists an initial condition* $\hat{x} \in \mathbb{R}^n$ *and a state sequence* $\{x_k\}_{k=0}^{N}$ *such that*

$$\begin{aligned} x_{k+1} &= Ax_k + Bu_k, \quad x_0 = \hat{x}, \\ y_k &= Cx_k + Du_k, \end{aligned}$$

for $k = 0,1,\dots,N-1$, *where* (A,B,C,D) *is a minimal realization of G.*

The goal is to describe all possible input-output trajectories of an LTI DT system, using one measured trajectory. Therefore, clearly the measured trajectory needs to contain enough information to be able to describe the input-output behavior of the system purely by data. In the LTI case, this informativity is characterized by persistency of excitation of the measurements input signal, which is defined as follows.

Definition 2.2 *A sequence* $\{c_k\}_{k=0}^{N-1}, c_k \in \mathbb{R}^q$, *is persistently exciting of order L, if* $\operatorname{rank}(H_L(c)) = qL$.

In other words, for c to be persistently exciting of order L, there have to exist qL linearly independent windows of length L in that sequence, implying a length $N > (q+1)L - 1$ for c. Therefore, for our purposes,

a signal is informative enough, if it is long enough and exciting enough, described by linear independence.

This informativity characterization is now used in the next result to provide a parametrization of all possible input-output trajectories of an unknown system using only one measured data trajectory. It was originally formulated in [38] in the behavioral context and has since been used in several data-driven publications, as mentioned in the introduction in Section 1.1, under the name *Fundamental Lemma*. It is explained in detail for state-space systems in [2] and proven in [33].

Theorem 2.1 ([2, Theorem 3]) *Suppose* $\{u_k,y_k\}_{k=0}^{N-1}$ *is a trajectory of an LTI system* G*, where* u *is persistently exciting of order* $L+n$*. Then,* $\{\bar{u}_k,\bar{y}_k\}_{k=0}^{L-1}$ *is a trajectory of* G *if and only if there exists* $\alpha \in \mathbb{R}^{N-L+1}$ *such that*

$$H_L(u,y)\alpha = \begin{pmatrix} \bar{u} \\ \bar{y} \end{pmatrix}, \quad \text{where} \quad H_L(u,y) = \begin{pmatrix} H_L(u) \\ H_L(y) \end{pmatrix}. \tag{2.1}$$

Theorem 2.1 is a powerful approach to replace the usual model by a representation using only one measured trajectory of the system. It can be used to build any input-output trajectory $(\bar{u},\bar{y})$ of length L of the system G, by taking linear combinations of windows of length L of the given measured trajectory (u,y). The if-direction follows from the fact that G is linear and hence any linear combination of trajectories of G results in a trajectory of G, i.e., persistence of excitation is not required for this direction. For the "only if"-direction, the input signal of the measured trajectory indeed has to be persistently exciting of order $L+n$ to guarantee existence of a suitable α for all trajectories of G. Intuitively speaking, the L degrees of freedom are required to span the whole input space and the additional n degrees of freedom account for the initial conditions. In conclusion, the stacked *Hankel* matrix in (2.1) spans the whole space of trajectories of length L of the system G.

Remark 2.1 *Theorem 2.1 can be extended to multiple, possibly not connected shorter, measurements, as shown in [33]. This reduces the requirements on the available measurements since none of the available inputs have to be persistently exciting. Moreover, the collection of the input measurements needs to be collectively persistently exciting, which is less restrictive then persistency of excitation for each individual input signal. Furthermore, collective persistency of excitation provides more flexibility in the length of the available measurements.*

Given our new system representation in the data-driven context by Theorem 2.1, it is now possible to employ it for a data-driven dissipativity characterization, which is presented in Section 2.2.

2.2. Data-driven dissipativity characterization

The classical dissipativity definition from [36, 37] involves the state variables of the system, which are assumed to be unknown in the present problem setup, while only input-output data is available. Therefore, the dissipativity definition from [12] in the input-output context is used, which reads as follows.

Definition 2.3 *The system G is dissipative w.r.t. the supply rate*

$$\Pi = \begin{pmatrix} Q & S \\ S^\top & R \end{pmatrix},$$

with $Q \in \mathbb{S}^m$, $R \in \mathbb{S}^p$ and $S \in \mathbb{R}^{m \times p}$, if

$$\sum_{k=0}^{r} \begin{pmatrix} u_k \\ y_k \end{pmatrix}^\top \Pi \begin{pmatrix} u_k \\ y_k \end{pmatrix} \geq 0, \quad \forall r \geq 0,$$

for all trajectories $\{u_k, y_k\}_{k=0}^{\infty}$ of G with initial condition $x_0 = 0$, where x is the state of an arbitrary minimal realization of G.

In [12] it is shown that this input-output definition is in fact equivalent to the definition by [37] for controllable LTI systems. Definition 2.3 only allows quadratic supply rates, but nevertheless covers important system properties, e.g., the $\mathcal{L}_2$-gain or passivity. The $\mathcal{L}_2$-gain γ of a system G can be found by the minimal $\hat{\gamma}$ such that the system is dissipative w.r.t. the supply rate

$$\Pi = \begin{pmatrix} \hat{\gamma}^2 I_m & 0_{m \times p} \\ 0_{p \times m} & -I_p \end{pmatrix} \tag{2.2}$$

and passivity of a system can be verified by checking dissipativity w.r.t. the supply rate

$$\Pi = \begin{pmatrix} 0_m & \frac{1}{2} I_m \\ \frac{1}{2} I_m & 0_m \end{pmatrix}.$$

In our data-driven setting, only finite input-output data is available, which results in a parametrization of finite-length trajectories and therefore a relaxed version of Definition 2.3, namely L-dissipativity, is introduced.

Definition 2.4 *The system G is L-dissipative w.r.t. the supply rate Π, if*

$$\sum_{k=0}^{r} \begin{pmatrix} u_k \\ y_k \end{pmatrix}^\top \Pi \begin{pmatrix} u_k \\ y_k \end{pmatrix} \geq 0, \quad \forall r = 0, \dots, L-1, \tag{2.3}$$

for all trajectories $\{u_k, y_k\}_{k=0}^{L-1}$ of G with initial condition $x_0 = 0$, where x is the state of an arbitrary minimal realization of G.

This definition leads to a finite-horizon dissipativity characterization in the input-output context. In [16] it is shown under weak assumptions that for $L \to \infty$, L-dissipativity is equivalent to infinite-horizon dissipativity as seen in Definition 2.3. From a practical point of view, it is sufficient to choose the horizon L large enough to obtain good approximations of the infinite-horizon case. In Definition 2.4, it is necessary that the inequality in (2.3) holds for all horizons $r = 0, \dots, L-1$. It was shown in [29] that in the LTI case, L-dissipativity is equivalent to inequality (2.3) holding only over the horizon L. This result is summarized in following proposition.

Proposition 2.1 ([29, Proposition 1]) *The LTI system G is L-dissipative w.r.t. the supply rate Π if and only if*

$$\sum_{k=0}^{L-1} \begin{pmatrix} u_k \\ y_k \end{pmatrix}^\top \Pi \begin{pmatrix} u_k \\ y_k \end{pmatrix} \geq 0, \tag{2.4}$$

for all trajectories $\{u_k, y_k\}_{k=0}^{L-1}$ of G with initial condition $x_0 = 0$, where x is the state of an arbitrary minimal realization of G.

The result follows from the fact that any trajectory of length L, with zero initial conditions and the first r steps zero in the input, can be split up in two parts. The first part of length r is a trajectory with zeros in both the input and the output and the second part can be seen as a new trajectory of length $L - r$ with zero initial conditions. Therefore, the first part can be neglected in (2.4) and it results that inequality (2.4) holds for the shorter horizon $L - r$.

Defining the stacked supply rate

$$\Pi_L = \begin{pmatrix} I_L \otimes Q & I_L \otimes S \\ I_L \otimes S^\top & I_L \otimes R \end{pmatrix} = \begin{pmatrix} Q_L & S_L \\ S_L^\top & R_L \end{pmatrix}, \tag{2.5}$$

condition (2.4) can be compactly rewritten as a vector-matrix product

$$\begin{pmatrix} u \\ y \end{pmatrix}^\top \Pi_L \begin{pmatrix} u \\ y \end{pmatrix} \geq 0. \tag{2.6}$$

In order to be able to parametrize all trajectories with zero initial conditions via Theorem 2.1, additional matrices are needed. First, the matrix

$$\tilde{V}_L^\nu = \begin{pmatrix} I_{m\nu} & 0_{m\nu\times m(L-\nu)} & 0_{m\nu\times p\nu} & 0_{m\nu\times p(L-\nu)} \\ 0_{p\nu\times m\nu} & 0_{p\nu\times m(L-\nu)} & I_{p\nu} & 0_{p\nu\times p(L-\nu)} \end{pmatrix} \in \mathbb{R}^{\nu(m+p)\times L(m+p)}, \tag{2.7}$$

for some positive integer $\nu \leq L$, is introduced. This implies for any trajectory $\{u_k,y_k\}_{k=0}^{L-1}$ of length L,

$$\tilde{V}_L^\nu \begin{pmatrix} u \\ y \end{pmatrix} = 0$$

if and only if

$$u_0 = \ldots = u_{\nu-1} = 0,$$
$$y_0 = \ldots = y_{\nu-1} = 0.$$

Therefore, the space of all trajectories of length L with the first ν entries equal to zero in both, the input and output, is equal to the image of $H_L(u,y)V_L^\nu(u,y)$, where

$$V_L^\nu(u,y) = (\tilde{V}_L^\nu H_L(u,y))^\perp. \tag{2.8}$$

In more detail, $V_L^\nu(u,y)$ is a basis matrix for the space

$$\{\alpha \in \mathbb{R}^{N-L+1} | \tilde{V}_L^\nu H_L(u,y)\alpha = 0\}$$

and therefore an input-output trajectory

$$\begin{pmatrix} \bar{u} \\ \bar{y} \end{pmatrix} = H_L(u,y)V_L^\nu(u,y)\beta, \tag{2.9}$$

with the first ν entries equal to zero, can be constructed by taking any $\beta \in \mathbb{R}^{\dim(\mathrm{col}(V_L^\nu(u,y)))}$.

Using these matrix definitions the main result of [29], the data-driven L-dissipativity characterization, can be stated.

Theorem 2.2 ([29, Theorem 2]) *Suppose $\{u_k,y_k\}_{k=0}^{N-1}$ is a trajectory of a DT LTI system G, where u is persistently exciting of order $L+n$. Then, for every ν with $n \leq \nu < L$, the system G is $(L-\nu)$-dissipative w.r.t. the supply rate Π if and only if*

$$V_L^\nu(u,y)^\top H_L(u,y)^\top \Pi_L H_L(u,y) V_L^\nu(u,y) \succcurlyeq 0. \tag{2.10}$$

Theorem 2.2 combines Theorem 2.1 and Proposition 2.1 by parametrizing the trajectories in (2.6) via the stacked *Hankel* matrices in (2.1) and the newly introduced basis matrix $V_L^\nu(u,y)$. One important aspect is the condition $n \leq \nu < L$, which guarantees that the image of $H_L(u,y)V_L^\nu(u,y)$ only contains trajectories with zero intial conditions since at least the first n (dimension of the state of an arbitrary minimal realization of G) entries in the input and the output of these trajectories are all zero. This is only possible if the initial conditions are zero, otherwise we would see a value different from zero in the n-th step in the output since the minimal realization implies observability of the system. Theorem 2.2 provides a data-driven condition for L-dissipativity in terms of a definiteness condition on one matrix, which is indeed easy to check with numerical methods. Based on this idea, using the *Fundamental Lemma* to parametrize all trajectories of an LTI system and using it for a data-driven dissipativity characterization, the next chapter shows how to verify closed-loop L-dissipativity for a given controller and available data of the plant in the standard feedback loop (Figure 1.2).

3. Data-driven controller validation for closed-loop dissipativity

In Chapter 2, a data-driven system representation of an open-loop system was presented and how one can use it to perform a finite-horizon dissipativity analysis on that system. The goal is now to transfer the general idea of the open-loop system analysis procedure to the standard feedback loop (see Figure 1.2). Given a model of the controller K and data of the plant G, it is possible to perform a dissipativity analysis on all closed-loop input-output channels $(r \mapsto z, r \mapsto e, r \mapsto u)$. Note that for the remainder of this thesis, only SISO systems are considered. To this end, given K and the measured trajectory of G, a parametrization of all closed-loop trajectories is presented by exploiting the commutativity property of SISO systems. This parametrization can be used for simulating an input signal r and to validate or invalidate the controller K for given L-dissipativity specifications for the closed loop. More precisely, necessary and sufficient conditons for closed-loop L-dissipativity for the channels $r \mapsto z$, $r \mapsto e$ and $r \mapsto u$ are provided.

The chapter is structured as follows. First, a general well-posedness assumption on the feedback loop for the developed framework and how to verify it in the data-driven context is presented. After disscusing the restrictiveness of this assumption, the mentioned parametrization of all closed-loop trajectories is introduced. Next, the possible applications of this parametrization are shown. First, it is applied for data-driven simulation and secondly it is shown how this parametrization yields a dissipativity characterization in form of a definiteness condition similar to the open-loop case. Finally, a comment on the applicability of this framework on multiple-input multiple-output (MIMO) systems and a numerical example conclude this chapter.

3.1. Well-posedness of the standard feedback loop

The setting in this chapter is as follows. A measured trajectory $\{u_k, y_k\}_{k=0}^{N-1}$ with persistently exciting input signal of the plant G and the finite-length

impulse response $\{g_k\}_{k=0}^{L-\nu-1}$ of the controller K are available. The need for the impulse response of the controller does not impose any restrictions on the framework at all, since in any model-based system representation the impulse response can either be computed or generated by simulation. For example, when K is given in the state-space by (A_c,B_c,C_c,D_c), the impulse response g can be calculated through the *Markov* parameters

$$\begin{aligned} g_0 &= D_c, \\ g_1 &= C_c B_c, \\ g_k &= C_c A_c^{k-1} B_c, \quad \text{for } k = 2,\dots,L-\nu-1. \end{aligned} \tag{3.1}$$

In order to be able to find a mathematical description of the standard feedback loop in Figure 1.2, we have to impose one condition on this interconnection. The interconnected system has to be well-posed, which is defined as follows.

Definition 3.1 ([10]) *The standard feedback loop (Figure 1.2) is well-posed, if all signals e, u and z in the feedback loop are uniquely defined for every choice of the system state variables for both, the controller K and the plant G, and every choice of the external input r.*

Well-posedness guarantees the existence of a unique response to every input. Without this condition we would not be able to describe the input-output behavior at all, since there can be multiple solutions to the same input. In conclusion, the well-posedness assumption is not a restriction on this framework, it is a necessity to be able to formulate it.

Well-posedness for LTI state-space systems can be ensured by using the following proposition.

Proposition 3.1 ([10]) *Suppose (A,B,C,D) is a realization of the SISO LTI plant G and (A_c,B_c,C_c,D_c) is a realization of the SISO LTI controller K. Then, the standard feedback loop is well-posed if and only if $1 + DD_c \neq 0$.*

Clearly, a simple sufficient condition for well-posedness is, if either the controller or the plant has no direct feedthrough term D. Furthermore, well-posedness also guarantees the existence of a well-defined closed-loop state-space realization, see [10]. In our data-driven setting, there is no state-space description for the plant G available, but Definition 2.1 ensures the existence of a realization describing the available data. Also for Proposition 3.1, only the feedthrough term D of the plant is needed, which can be

calculated using the presented results. To this purpose, one can use Theorem 2.1, i.e., equation (2.9) with $\nu \geq n$, where n is the dimension of the state of an arbitrary minimal realization of G, to construct an input-output trajectory of G with zero initial conditions

$$\begin{pmatrix} \tilde{u} \\ \tilde{y} \end{pmatrix} = H_L(u,y) V_L^{\nu}(u,y) \beta$$

such that $\tilde{u}_\nu \neq 0$, by choosing an appropriate β. Now, one can directly calculate the feedthrough term by

$$D = \frac{\tilde{y}_\nu}{\tilde{u}_\nu},$$

since $(\tilde{u},\tilde{y})$ is a trajectory with zero intial conditions and both, the input and the output are zero the first ν entries. The feedthrough term D_c of the controller K can be read of by using the dependency in (3.1) from the given impulse response g and therefore we can check well-posedness of the standard feedback loop by applying Proposition 3.1. Now we can assure that all signals in the standard feedback loop are uniquely defined in our data-driven setting and develop a description of all closed-loop trajectories.

3.2. Trajectory-based representation of the closed loop

In this section, the closed-loop data-driven trajectory parametrization is stated. The setting is as described in Section 3.1, the model of the controller K and a measured trajectory of the plant G with persistently exciting input signal are available. To this end, Theorem 2.1 will be naturally extended to the feedback interconnection case, by exploiting the fact that SISO LTI systems are commutative when dealing with trajectories corresponding to zero initial conditions. Therefore, we obtain a single matrix for each channel $r \mapsto z$, $r \mapsto e$ and $r \mapsto z$, which span the whole trajectory space of that channel. For a clearer structure, only the channel $r \mapsto z$ is extensively studied since the other channels follow exactly the same procedure.

The main result of this section, the closed-loop trajectory parametrization, reads as follows.

Proposition 3.2 *Suppose the standard feedback loop in Figure 1.2 is well-posed. Let $\{u_k,y_k\}_{k=0}^{N-1}$ be a trajectory of G, where u is persistently exciting of order $L+n$, and $\{g_k\}_{k=0}^{L-\nu-1}$ be the finite-length impulse response of the controller K.*

Then, for any ν with $n \leq \nu < L$, $\{r_k,z_k\}_{k=0}^{L-\nu-1}$ is a closed-loop trajectory of the standard feedback loop with zero initial conditions if and only if there exists a vector $\beta \in \mathbb{R}^{\dim(\mathrm{col}(V_L^\nu(u,y)))}$ such that

$$M_{L-\nu}(g)J_L^\nu H_L(u,y)V_L^\nu(u,y)\beta = \begin{pmatrix} r \\ z \end{pmatrix}, \tag{3.2}$$

where

$$M_{L-\nu}(g) = \begin{pmatrix} I_{L-\nu} & T(g) \\ 0_{L-\nu} & T(g) \end{pmatrix}$$

and

$$J_L^\nu = \begin{pmatrix} \tilde{J}_L^\nu & 0_{(L-\nu)\times L} \\ 0_{(L-\nu)\times L} & \tilde{J}_L^\nu \end{pmatrix} \quad \textit{with} \quad \tilde{J}_L^\nu = \begin{pmatrix} 0_{(L-\nu)\times\nu} & I_{L-\nu} \end{pmatrix}.$$

Proof if: For a fixed $\beta \in \mathbb{R}^{\dim(\mathrm{col}(V_L^\nu(u,y)))}$

$$H_L(u,y)V_L^\nu(u,y)\beta = \begin{pmatrix} \bar{u} \\ \bar{y} \end{pmatrix} \tag{3.3}$$

is an input-output trajectory of length L of G with $\bar{u}_0 = \ldots = \bar{u}_{\nu-1} = 0$ and $\bar{y}_0 = \ldots = \bar{y}_{\nu-1} = 0$, by using Theorem 2.1 combined with the definition (2.8) of $V_L^\nu(u,y)$. Since $\nu \geq n$ by assumption, $(\bar{u},\bar{y})$ is a trajectory of G with $\bar{x}_k = 0$ for $k = 0,\ldots,\nu-1$, where $\bar{x}$ is the corresponding state in some minimal realization. Multiplying (3.3) with J_L^ν from the left yields

$$J_L^\nu H_L(u,y)V_L^\nu(u,y)\beta = \begin{pmatrix} \tilde{J}_L^\nu & 0_{(L-\nu)\times L} \\ 0_{(L-\nu)\times L} & \tilde{J}_L^\nu \end{pmatrix} \begin{pmatrix} \bar{u} \\ \bar{y} \end{pmatrix} = \begin{pmatrix} \hat{u} \\ \hat{y} \end{pmatrix}, \tag{3.4}$$

where $(\hat{u},\hat{y})$ contains the last $L-\nu$ entries of $(\bar{u},\bar{y})$ and is therefore a trajectory of length $L-\nu$ of G with zero initial conditions. Representing the controller K via the *Toeplitz* matrix $T(g)$ implies also zero initial conditions by assumption for the controller. Therefore, using the commutativity of SISO LTI systems with zero initial conditions, the standard feedback loop has the same input-output behavior from $r \mapsto z$ as the transformed loop shown in Figure 3.1. Multiplying (3.4) by $M_{L-\nu}(g)$ from the left, we obtain

$$M_{L-\nu}(g)J_L^\nu H_L(u,y)V_L^\nu(u,y)\beta = M_{L-\nu}(g)\begin{pmatrix} \hat{u} \\ \hat{y} \end{pmatrix}.$$

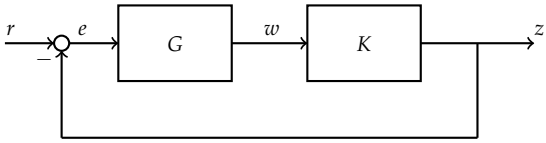

Figure 3.1.: Standard feedback loop with interchanged controller and plant.

Using the signal definition of the interchanged standard feedback loop in Figure 3.1 leads to

$$\begin{aligned} M_{L-\nu}(g)\begin{pmatrix}\hat{u}\\ \hat{y}\end{pmatrix} = M_{L-\nu}(g)\begin{pmatrix}\hat{e}\\ \hat{w}\end{pmatrix} &= \begin{pmatrix}\hat{e}+T(g)\hat{w}\\ T(g)\hat{w}\end{pmatrix} \\ &= \begin{pmatrix}\hat{e}+\hat{z}\\ \hat{z}\end{pmatrix} \\ &= \begin{pmatrix}\hat{r}\\ \hat{z}\end{pmatrix}, \end{aligned} \tag{3.5}$$

where $\hat{e} = \hat{u}$, $\hat{w} = \hat{y}$ and $\hat{z} = T(g)\hat{w}$. Since the closed loop is well-posed, we can construct a state-space realization of the resulting closed loop by stacking the states of an arbitrary realization of the controller and the states of an arbitrary realization of the plant. As we assumed zero initial conditions for both, the controller and the plant, also the constructed closed-loop realization has zero initial conditions. Therefore, $(\hat{r},\hat{z})$ is a trajectory of length $L-\nu$ of the closed loop with zero initial conditions, which, together with (3.5), concludes the "if"-part.

Only if: Suppose $\{\hat{r}_k,\hat{z}_k\}_{k=0}^{L-\nu-1}$ is a closed-loop trajectory of the standard feedback loop (Figure 1.2) with zero initial conditions. Since a closed-loop state-space realization can be constructed by stacking the individual states of realizations of K and G, zero initial conditions for the closed loop imply zero initial conditions for both, the controller and the plant. Similar to the if-part, we use the commutativity property and reverse the steps seen in (3.5) to guarantee the existence of a trajectory $(\hat{u},\hat{y})$ of length $L-\nu$ of G with zero initial conditions, which satisfies (3.5). Hence, we can artificially insert zeros

to deduce that

$$\begin{pmatrix} \bar{u} \\ \bar{y} \end{pmatrix} = \begin{pmatrix} 0_{\nu \times 1} \\ \hat{u} \\ 0_{\nu \times 1} \\ \hat{y} \end{pmatrix}$$

is a trajectory of length L of G. Thus, using Theorem 2.1 and the definition (2.8) of $V_L^{\nu}(u,y)$, there exists a vector β satisfying (3.2). ■

Proposition 3.2 is a natural extension of Theorem 2.1, which allows us to parametrize all closed-loop trajectories by one single matrix (see (3.2)). The introduced parametrization is linear in the controller parameters, which is an essential fact to perform controller synthesis (Chapter 4). As mentioned above, not only the channel $r \mapsto z$ can be considered, but also all other input-output pairs. The following remark gives more details about the other available channels.

Remark 3.1 *Similar to Proposition 3.2, it is possible to parametrize closed-loop input-output trajectories corresponding to further channels, for instance $r \mapsto e$ (reference to error) or $r \mapsto u$ (reference to control variable). To this purpose, one has to change the matrix $M_{L-\nu}(g)$ in (3.2). For the channels $r \mapsto e$ and $r \mapsto u$, Proposition 3.2 holds with*

$$M_{L-\nu}(g) = \begin{pmatrix} I_{L-\nu} & T(g) \\ I_{L-\nu} & 0_{L-\nu} \end{pmatrix} \tag{3.6}$$

and

$$M_{L-\nu}(g) = \begin{pmatrix} I_{L-\nu} & T(g) \\ T(g) & 0_{L-\nu} \end{pmatrix}, \tag{3.7}$$

respectively. The proof for these channels goes along the same lines as for $r \mapsto z$.

Since we are now able to construct all input-output trajectories of the standard feedback loop, we can use Proposition 3.2 for data-driven simulation (Section 3.3) and a dissipativity analysis on the standard feedback loop (Section 3.4).

3.3. Closed-loop simulation

Simulation, the calculation of the output signal of a system for a given input signal and an initial condition, is a widely used tool in system analysis as well

as in controller design. In the data-driven context, [21] provides an approach for closed-loop data-driven simulation for a controller in minimal kernel representation. With Proposition 3.2, on the other hand, it is possible to perform simulation of the closed loop similar to the idea in [23] for an open-loop LTI system using Theorem 2.1. However, Proposition 3.2 is restricted to trajectories with zero initial conditions. Following result summarizes the data-driven simulation for trajectories in the standard feedback loop.

Proposition 3.3 *Suppose the standard feedback loop in Figure 1.2 is well-posed. Let* $\{u_k,y_k\}_{k=0}^{N-1}$ *be a trajectory of* G*, where* u *is persistently exciting of order* $L+n$*, and* $\{g_k\}_{k=0}^{L-\nu-1}$ *be the finite-length impulse response of the controller* K*. Then, for any* ν *with* $n \leq \nu < L$ *and any reference signal* $\{\tilde{r}_k\}_{k=0}^{L-\nu-1}$*, there exists a unique output* $\{\tilde{z}\}_{k=0}^{L-\nu-1}$ *of the closed loop. The output* $\tilde{z}$ *corresponding to zero initial conditions, can be calculated by solving following system of equations*

$$E_L^\nu(u,y,g)\beta = (\tilde{J}_L^\nu H_L(u)V_L^\nu(u,y) + T(g)\tilde{J}_L^\nu H_L(y)V_L^\nu(u,y))\beta = \tilde{r} \tag{3.8}$$

for β *and plug it into*

$$\tilde{z} = T(g)\tilde{J}_L^\nu H_L(y)V_L^\nu(u,y)\beta. \tag{3.9}$$

Proof By the well-posedness assumption of the feedback loop, the existence of a unique response $\tilde{z}$ to any input $\tilde{r}$ and arbitrary initial condition is guaranteed. It remains to show that (3.8) is always solvable when considering zero inital conditions and (3.9) leads to the corresponding output of the feedback loop. Well-posedness and persistence of excitation of the input signal u of the data trajectory of the plant G guarantee the existence of a, possibly non-unique, β for equation (3.8), which is shown now.

Defining $T(g_G)$ as the lower-triangular *Toeplitz* matrix of the impulse response $\{g_{G,k}\}_{k=0}^{L-1}$ of length L, containing the *Markov* parameters (see (3.1)) obtained from any minimial realization (A,B,C,D) of the plant G, $E_L^\nu(u,y,g)$

in the left-hand side of (3.8) can be reformulated into

$$
\begin{aligned}
&E_L^\nu(u,y,g) = \\
&= \tilde{J}_L^\nu H_L(u) V_L^\nu(u,y) + T(g)\tilde{J}_L^\nu H_L(y) V_L^\nu(u,y) \\
&= (\tilde{J}_L^\nu + T(g)\tilde{J}_L^\nu T(g_G)) H_L(u) V_L^\nu(u,y) \\
&= \left(\begin{pmatrix} 0_{(L-\nu)\times\nu} & I_{L-\nu} \end{pmatrix} + \begin{pmatrix} \star & \cdots & \cdots & \star & D_cD & 0 & \cdots & 0 \\ \vdots & \ddots & \ddots & \vdots & \star & \ddots & \ddots & \vdots \\ \vdots & \ddots & \ddots & \vdots & \vdots & \ddots & D_cD & 0 \\ \star & \cdots & \cdots & \star & \star & \cdots & \star & D_cD \end{pmatrix} \right) H_L(u) V_L^\nu(u,y) \\
&= \begin{pmatrix} \star & \cdots & \cdots & \star & 1+D_cD & 0 & \cdots & 0 \\ \vdots & \ddots & \ddots & \vdots & \star & \ddots & \ddots & \vdots \\ \vdots & \ddots & \ddots & \vdots & \vdots & \ddots & 1+D_cD & 0 \\ \star & \cdots & \cdots & \star & \star & \cdots & \star & 1+D_cD \end{pmatrix} H_L(u) V_L^\nu(u,y),
\end{aligned}
$$

where $\star$ denotes irrelevant entries. Recall, that the first ν rows in $H_L(u)V_L^\nu(u,y)$ are zero and therefore we can further rewrite $E_L^\nu(u,y,g)$ into

$$
E_L^\nu(u,y,g) = \underbrace{\begin{pmatrix} 1+D_cD & 0 & \cdots & 0 \\ \star & \ddots & \ddots & \vdots \\ \vdots & \ddots & 1+D_cD & 0 \\ \star & \cdots & \star & 1+D_cD \end{pmatrix}}_{\tilde{E}} \underbrace{\tilde{J}_L^\nu H_L(u) V_L^\nu(u,y)}_{\hat{E}}.
$$

Since we assumed well-posedness, $1 + D_cD \neq 0$ by Proposition 3.1 and therefore $\tilde{E}$ has full rank. Furthermore, u is persistently exciting of order $L + n$, and hence the image of $\hat{E}$ contains all input signals of length $L - \nu$, i.e., $\mathrm{col}(\hat{E}) = \mathbb{R}^{L-\nu}$, implying full row rank for $\hat{E}$. In conclusion, the product $E_L^\nu(u,y,g) = \tilde{E}\hat{E}$ has full row rank implying solvability of equation (3.8).

Further, we have to show that (3.9) yields the output of the feedback loop when plugging in the obtained β while solving (3.8). Note that (3.8) is equivalent to the upper block row condition in (3.2) from Proposition 3.2. Using Proposition 3.2 the corresponding output has to satisfy the lower block row condition in (3.2), which is equivalent to (3.9) and therefore concludes the proof. ∎

Remark 3.2 *Based on Remark 3.1, closed-loop simulation, as summarized in Proposition 3.3, is also possible for the other known input-output channels.*

Note that $V_L^\nu(u,y) \in \mathbb{R}^{2L\times 2(L-\nu)}$, resulting in a wide matrix $E_L^\nu(u,y,g)$, provides additional freedom in β, which can be exploited to further specify the desired resulting β when solving (3.8). This is especially valuable when the data (u,y) of the plant is affected by noise, which is in practice always the case. Hence, additional regularization terms for β can counteract overfitting for the present noise. Useful examples for regularizer are, e.g., l_1-norm regularization, which yields a sparse β, or l_2-norm regularization, which yields the β with the smallest energy. Considering the l_2-norm regularization, the resulting quadratic program in β, for solving (3.8), would exemplarily read

$$\min_{\beta} \|E_L^\nu(u,y,g)\beta - \tilde{r}\|_2^2 + \lambda\|\beta\|_2^2, \tag{3.10}$$

where $\lambda \in \mathbb{R}$ is the regularization parameter. This design parameter λ can be used to determine the relative importance of the regularization term $\|\beta\|_2^2$ compared to the error term$\left\|E_L^\nu(u,y,g)\beta - \tilde{r}\right\|_2^2$, depending on the available data. For further details about regression and regularization the reader is refered to [5].

In summary, Proposition 3.3 can be used to simulate the output of the standard feedback loop for a given input reference, which can be applied for validating the performance of a given controller. In addition, in Section 3.4, the main result of this chapter is presented, where Proposition 3.2 is used to validate L-dissipativity for the closed loop in a similar fashion as done in Theorem 2.2.

3.4. Closed-loop dissipativity validation

Now the main result of this chapter, the closed-loop data-driven finite-horizon dissipativity characterization for an unknown plant G and a given controller K in the standard feedback loop (Figure 1.2) is presented. Necessary and sufficient conditions for L-dissipativity in terms of one definiteness condition of a single matrix are provided.

Exploiting the advantages of Proposition 3.2 results in the following theorem.

Theorem 3.1 *Suppose the standard feedback loop in Figure 1.2 is well-posed. Let* $\{u_k,y_k\}_{k=0}^{N-1}$ *be a trajectory of G, where u is persistently exciting of order $L+n$,*

and $\{g_k\}_{k=0}^{L-\nu-1}$ *be the finite-length impulse response of the controller* K*. Then, for any* ν *with* $n \leq \nu < L$*, the channel* $r \mapsto z$ *is* $(L-\nu)$*-dissipative w.r.t. the supply rate* Π *if and only if*

$$V_L^\nu(u,y)^\top H_L(u,y)^\top J_L^{\nu\top} M_{L-\nu}(g)^\top \Pi_{L-\nu} M_{L-\nu}(g) J_L^\nu H_L(u,y) V_L^\nu(u,y) \succcurlyeq 0, \tag{3.11}$$

where

$$M_{L-\nu}(g) = \begin{pmatrix} I_{L-\nu} & T(g) \\ 0_{L-\nu} & T(g) \end{pmatrix}.$$

Proof By using the dissipativity condition (2.4) in the rewritten form (2.6), the closed loop from $r \mapsto z$ is $(L-\nu)$-dissipative w.r.t. the supply rate Π if and only if

$$\begin{pmatrix} r \\ z \end{pmatrix}^\top \Pi_{L-\nu} \begin{pmatrix} r \\ z \end{pmatrix} \geq 0.$$

for all trajectories (r,z) of length $L-\nu$ with zero initial conditions. Furthermore, using Proposition 3.2, this turns out to be equivalent to (3.11). ■

Theorem 3.1 provides a validation technique for closed-loop $(L-\nu)$- dissipativity in the standard feedback loop. The provided definiteness condition (3.11) can easily be checked numerically and therefore is a simple tool for verifying dissipativity. As for Proposition 3.2, it is possible to obtain closed-loop dissipativity conditions for other channels by using the appropriate matrix $M_{L-\nu}(g)$ as discussed in Remark 3.1. The main advantage of this result, compared to applying Theorem 2.2 to closed-loop data, is that the controller K does not have to be implemented and no new measurements have to be taken. One single measurement of the plant allows us to validate all possible controllers. This is indeed a very important aspect since this allows us to perform controller synthesis via finite-horizon dissipativity specifications directly from the available data of the plant G by solving a QMIFP (see Chapter 4).

3.5. Comment on MIMO systems

In the introduction to Chapter 3, it was stated that only SISO systems are considered, which is due to the fact that MIMO systems are not commutative in general and this property is used in the trajectory parametrization

in Proposition 3.2. The SISO-assumption was only made to guarantee the commutativity of the plant and the controller. Hence, the framework could be formulated in a more general manner, including all LTI DT commutative systems. Nevertheless, when not restricted to the SISO case, it is not straightforward to guarantee this commutativity property in the data-driven setting without a model for the plant G. There is a workaround available, which does include the identification of the input-output map to some extent, more precisely the *Toeplitz* matrix of the impulse response of the plant G. The general idea is sketched in the following, but not extensively studied since there are more robust and advanced methods available to identify the input-output map of a system in the system identification literature (see [20]). To this purpose, we pick out columns from the data-driven system representation (2.9) of an open-loop system, such that the upper part, corresponding to u, is invertible. This allows us to come up with an explicit equation for the output y in terms of the input u.

Given a trajectory (u,y) of the plant G with persistently exciting input signal u of order $L+n$, recall that

$$\begin{aligned}\begin{pmatrix}\tilde{u}\\ \tilde{y}\end{pmatrix} &= \begin{pmatrix}\begin{pmatrix}0_{m(L-\nu)\times m\nu} & I_{m(L-\nu)}\end{pmatrix} H_L(u)V_L^\nu(u,y)\\ \begin{pmatrix}0_{p(L-\nu)\times p\nu} & I_{p(L-\nu)}\end{pmatrix} H_L(y)V_L^\nu(u,y)\end{pmatrix}\beta\\ &= \begin{pmatrix}N_u(u,y)\\ N_y(u,y)\end{pmatrix}\beta,\end{aligned}$$

with $\nu \geq n$ and any β, is a trajectory of length $L-\nu$ with zero initial conditions. Taking now $m(L-\nu)$ linearly independent columns with indices $c = \begin{pmatrix}c_0 & \cdots & c_{m(L-\nu)-1}\end{pmatrix}$ out of $N_u(u,y)$, e.g., by calculating the row reduced echelon form and taking the pivot column indices, we can construct the following matrices

$$\begin{aligned}N_u^r(u,y) &= N_u(u,y)[:,c],\\ N_y^r(u,y) &= N_y(u,y)[:,c],\end{aligned}$$

where $[:,c]$ denotes the submatrix containing all rows and the columns with indices defined in c. Since our chosen columns c from $N_u(u,y)$ are linearly independent, the matrices $N_u^r(u,y)$ and $N_y^r(u,y)$ contain all the necessary information to construct new trajectories via

$$\begin{pmatrix}\tilde{u}\\ \tilde{y}\end{pmatrix} = \begin{pmatrix}N_u^r(u,y)\\ N_y^r(u,y)\end{pmatrix}\beta^r.$$

Therefore, for a given input $\tilde{u}$ we can calculate the corresponding output by

$$\tilde{y} = N_y^r(u,y)N_u^r(u,y)^{-1}\tilde{u} = T(g_G)\tilde{u}.$$

More precisely, we can determine the *Toeplitz* matrix of the finite-length impulse response g_G of the plant G by $T(g_G) = N_y^r(u,y)N_u^r(u,y)^{-1}$. Note that the necessary inversion can be very sensitive w.r.t. noise and is thus impractical. Once the input-output map of the plant is available, one can either check commutativity by following assertion

$$T(g)T(g_G) = T(g_G)T(g)$$

and apply the introduced framework in this thesis or on the other hand use this input-output map directly for analysis of the closed loop. In conclusion, the in Chapter 3 presented results can be extended to commutative MIMO systems. However, checking commutativity for non SISO systems is not straightforward without identifying a model of the plant and therefore cannot be seen as a direct data-driven method.

3.6. Numerical example

To conclude this chapter, the presented results, especially the use of Proposition 3.2 in Section 3.3 and Section 3.4, are applied to an example system to perform data-driven analysis on the closed loop. More precisely, it is shown how these results can be used to, first, simulate the closed-loop step response in Section 3.6.1, and secondly, how the $\mathcal{L}_2$-gain from $r \mapsto z$ of the feedback interconnection can be approximated by a finite-horizon dissipativity specification in Section 3.6.2. The numerical calculations were all performed in *Matlab*.

To this purpose, following random example plant G

$$\begin{aligned} x_{k+1} &= \begin{pmatrix} 0.3637 & -0.0625 & -0.4839 \\ -0.4745 & 0.3945 & 0.1415 \\ -0.1136 & 0.4912 & 0.4620 \end{pmatrix} x_k + \begin{pmatrix} 0 \\ -1.2701 \\ 1.1752 \end{pmatrix} u_k \\ y_k &= \begin{pmatrix} 2.0292 & 0 & 0.6037 \end{pmatrix} x_k \end{aligned}$$

has been generated, by using the command $\mathrm{drss}(3,1,1)$ with a seed of $\mathrm{rng}(1)$. Additionally, the feedtrough term has been set to $D = 0$, due to simplifications when designing a suitable controller via LMI techniques (see [31]).

These LMI techniques for continous-time system were transfered to discrete-time systems and used to design a suitable controller for the example plant G, where following controller

$$x_{c,k+1} = \begin{pmatrix} 0.1661 & 0.0626 & -0.3206 & 0.1229 \\ -2.8036 & 2.6432 & 3.3166 & 2.0776 \\ 2.1072 & -1.5541 & -2.3887 & -1.8661 \\ -0.0082 & -0.0064 & -0.0138 & 0.9940 \end{pmatrix} x_{c,k} + \begin{pmatrix} -0.0157 \\ -0.5686 \\ 0.4511 \\ -0.2455 \end{pmatrix} u_k,$$

$$y_{c,k} = \begin{pmatrix} -1.9041 & 1.7464 & 2.4391 & 1.6098 \end{pmatrix} x_{c,k} + (-0.3932) u_{c,k}.$$

was obtained.

3.6.1. Step response simulation

In this section, the closed-loop step response for the mentioned plant G and controller K is calculated through the data-driven closed-loop simulation, shown in Section 3.3, i.e, we have to solve (3.8) for β when choosing r as the step input and plug it into (3.9) to yield the corresponding output. After that, the same procedure is repeated while considering noisy measurements, and it is illustrated how the mentioned regularization (3.10) can counteract the noise and lead to quite good results. Therefore, we assume the model of the plant G is unknown to us and only an input-ouput trajectory (u,y) is available. This trajectory $\{u_k,y_k\}_{k=0}^{N-1}$ of length $N = 559$ was generated by simulating the model of G with a persistently exciting input u of order $L+n$, where the horizon was chosen $L = 140$ and the dimension of the state is $n = 3$. The persistently exciting input u was created by using the $\mathrm{rand}(N,1)$ command with a seed $\mathrm{rng}(1)$, which yields a vector containing pseudorandom values from the standard uniform distribution between 0 and 1. By shifting the vector via $u = u - 0.5\mathrm{ones}(N,1)$ and scaling it afterwards by $u = 20u$, we get a random persistently exciting vector u containing values in the interval $[-10,10]$. With the available input-output trajectory (u,y), one can calculate the corresponding *Hankel* matrices $H_L(u)$ and $H_L(y)$. Next, the matrix $V_L^\nu(u,y)$ can be calculated by $V_L^\nu(u,y) = \mathrm{null}(\tilde{V}_L^\nu H_L(u,y))$, where ν needs to be an upper bound on the plants state dimension. Since we know the dimension exactly we can choose $\nu = n$. Afterwards, the impulse response $\{g_k\}_{k=0}^{L-\nu-1}$ of the controller is calculated via (3.1). Finally, to solve (3.8) for β with $r = \mathrm{ones}(L-\nu,1)$, we use the least-squares solution which can be obtained in *Matlab* by $\beta = (E_L^\nu(u,y,g)^\top E_L^\nu(u,y,g))\backslash(E_L^\nu(u,y,g)^\top r)$. The

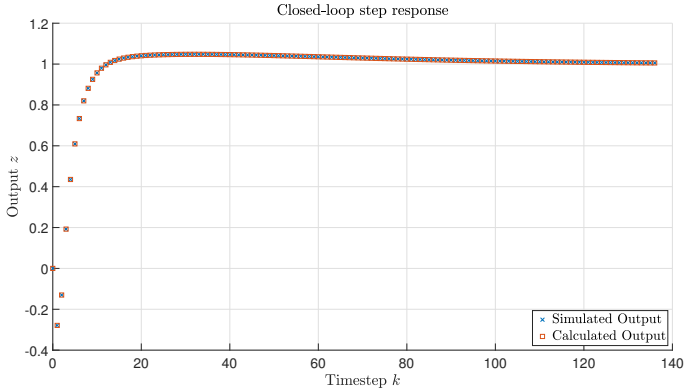

Figure 3.2.: Step response from $r \mapsto z$.

corresponding output

$$z = T(g)\tilde{J}_L^{\nu} H_L(y) V_L^{\nu}(u,y)\beta$$

for the step input is shown in Figure 3.2. Figure 3.2 also shows the step response obtained from simulating the closed loop via the available models, and it can be seen that both outputs, the calculated one and the simulated one, coincide perfectly. Hence, our data-driven closed-loop simulation works as expected.

Since in real word problems data is never clean and always affected by some noise, the impact of noise for data-driven simulation is shown in the following. Therefore, the available trajectory (u,y) of the plant is artificially corrupted by output noise, i.e., we can only measure the noisy output $\tilde{y} = y + 2\theta(\text{rand}(N,1) - 0.5\text{ones}(N,1)$ for the input u of the plant G, where θ represents the maximal amplitude of the noise. Now, the above described procedure of calculating the step output of the closed loop is done for $\theta = 0.1$ and $\theta = 0.5$ by using the input-output trajectory $(u,\tilde{y})$ instead of (u,y). The results can bee seen in Figure 3.3. As expected, the calculated outputs from our data-driven simulation from noisy measurements differ from the true output of the closed loop. As one would expect, the difference between the true signal and the calculated signal increases with increasing θ, which can be seen in Figure 3.3. For $\theta = 0.5$ there exist big spikes far away from the

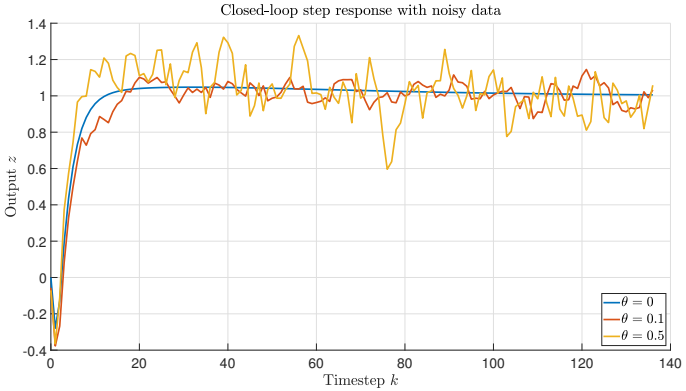

Figure 3.3.: Step response from $r \mapsto z$ with noisy measurement (u,y).

true signal. As mentioned in Section 3.3, regularization can be used to yield better results even when the data is affected by noise. To show the effect of regularization, the noisy measurement $(u,\tilde{y})$ with $\theta = 0.5$ has been used and the optimization problem (3.10) was solved for β for various regularization parameters λ. The solution to the optimization problem can be obtained in *Matlab* by $\beta = (E_L^v(u,y,g)^\top E_L^v(u,y,g) + \lambda I) \backslash (E_L^v(u,y,g)^\top r)$ for one specific λ. The corresponding calculated output z is illustrated in Figure 3.4. Naturally, for $\lambda = 0$ the calculation yields the same results as seen in Figure 3.3 for $\theta = 0.5$. However, when increasing to $\lambda = 0.5$, the data-driven simulation results nearly in a perfect fit compared to the true simulated step response from the model. This is a remarkable result, since we were able to construct nearly the true step response from noisy data by a purely data-driven simulation method. To be fair, the selection of a suitable λ is without the knowledge of the actual response not straightforward. The general heuristic is to increase the regularization parameter until the curve is smooth enough. When increasing λ too much, the response starts to drift away resulting in a flattened curve (see Figure 3.4, $\lambda = 10000$) since the regularization term in (3.10) gets increasingly important, hence decreasing the norm of β more and more. Overall, the introduced data-driven simulation method for the standard feedback loop works remarkably well, even when the measured data is affected by noise, where regularization can help to improve the

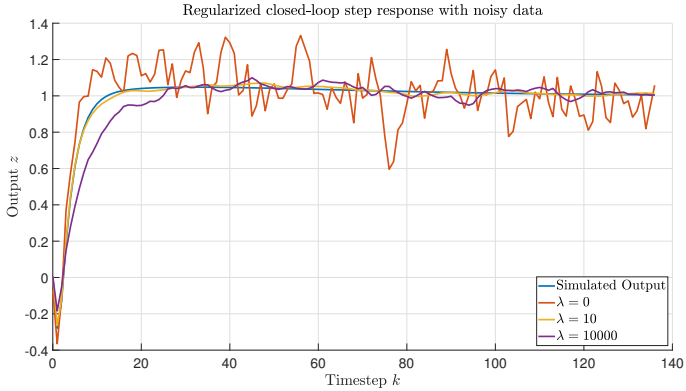

Figure 3.4.: Step response from $r \mapsto z$ with regularization by λ.

results.

3.6.2. $\mathcal{L}_2$-gain approximation via dissipativity analysis

After showing an example for simulation, we take advantage of the data-driven L-dissipativity analysis framework for the closed loop from Section 3.4 to approximate the $\mathcal{L}_2$-gain from $r \mapsto z$. The influence of the horizon $L - \nu$ is examined for the quality of the approximation for the example plant and controller mentioned at the beginning of the section. To this purpose, the minimal γ has to be found such that the closed loop from $r \mapsto z$ is $L - \nu$ dissipative w.r.t. the supply rate

$$\Pi = \begin{pmatrix} \gamma^2 & 0 \\ 0 & -1 \end{pmatrix}$$

as defined in (2.2). This can be done by a simple bisection algorithm over γ with the condition

$$V_L^\nu(u,y)^\top H_L(u,y)^\top J_L^{\nu\top} M_{L-\nu}(g)^\top \Pi_{L-\nu} M_{L-\nu}(g) J_L^\nu H_L(u,y) V_L^\nu(u,y) \succcurlyeq 0$$

for each iteration. To this end, we collect again an input-output trajectory (u,y) of the plant G and construct all necessary matrices as described at the beginning of Section 3.6.1. Then, we run this bisection algorithm multiple

times for different values of L. Starting at $L = \nu$ and increasing L until $L = 200$. The minimal γ, and therefore the $\mathcal{L}_2$-gain approximation, for the closed loop over the different horizons L are plotted in Figure 3.5 (labeled "plant data"). It can be seen that the approximation approaches the true

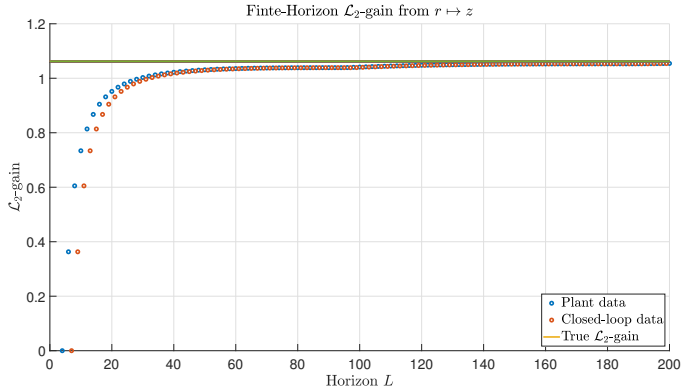

Figure 3.5.: $\mathcal{L}_2$ approximation $r \mapsto z$ over the horizon L.

$\mathcal{L}_2$-gain quickly for small L, but then slows down and barely changes over a wide range of horizons. Only from $L = 100$ upwards the approximation starts to get more accurate again and at $L = 200$ nearly reaches the true value. Note that the quality of the approximation in regard to the horizon depends heavily on the system and therefore it cannot be concluded that for all systems a horizon of, e.g., $L = 60$ yields good results. Indeed, it is remarkable that this seemingly low horizon works suprisingly well. For comparison reasons, Figure 3.5 also shows the approximation of the $\mathcal{L}_2$-gain, when applying Theorem 2.2 to closed-loop data (labeled "closed-loop data"). It can be seen that both methods converge almost equally fast to the true value, although the method introduced in Section 3.4 is a little faster, since for the same horizon L, Theorem 3.1 can guarantee dissipativity over the horizon $L - \nu$ with $\nu = n = 3$, whereas Theorem 2.2 can only guarantee dissipativity over the horizon $L - \nu$ with $\nu = n + n_c = 7$, where $n_c = 4$ is the state dimension of the controller K. This little advantage of Theorem 3.1 is most noticeable for small horizons (compare Figure 3.5). However, mentioning again, for Theorem 2.2, it was necessary to collect closed-loop

data by implementing the controller K, which was obsolete for Theorem 3.1, the main aspect why this theorem can be extended to a controller synthesis framework as presented in Chapter 4. In conclusion, this example demonstrates the applicability of Theorem 3.1 to perform a dissipativity analysis, in the form of an $\mathcal{L}_2$-gain approximation, on the closed loop on the basis of plant data and a model of the controller.

4. Data-driven controller synthesis for closed-loop dissipativity

Using the framework in Chapter 3, one can perform analysis on the standard feedback loop using a single measurement of the plant and a model of the controller. In this chapter, the data-driven analysis framework is extended to a controller synthesis framework. Given a measurement of the plant G, the goal is to design a controller such that given finite-horizon dissipativity specifications for the closed loop are met. This dissipativity conditions can be used to design meaningful controller depending on the corresponding use case. For example, the theory of mixed-sensitivity design [17] can be formulated in dissipativity conditions and used for loopshaping for reference tracking control. However, also many other well-known dissipativity conditions can be imposed on the closed loop for controller design. In a first step, in Section 4.1, the dissipativity analysis inequality from Section 3.4 is reformulated into a synthesis inequality in terms of a QMI in the controller parameters. This resulting QMI has to be solved to yield a satisfying controller, which is done in Section 4.2. After summarizing the general data-driven controller design procedure in Section 4.3, including useful design specifications as well as multi-objective design, the procedure is applied to an example system in Section 4.4.

4.1. Synthesis inequality

The setting is as follows: An input-output trajectory (u,y) with persistently exciting input u of the plant G is available. Furthermore, a finite-horizon dissipativity specification for the closed loop in terms of a supply rate Π and an horizon L is given. The goal is to find a finite-length impulse response $\{g_k\}_{k=0}^{L-\nu-1}$ of the controller such that the closed loop is dissipative w.r.t. the supply rate Π. As already mentioned in Section 3.2, one advantage of the closed-loop trajectory representation (3.2) is the linear dependence of the controller parameters. This allows us to reformulate the dissipativity analysis inequality (3.11) into a QMI in the controller parameters. Beforehand,

we impose some structure for the controller, which first guarantees causality of the controller and gives us the opportunity to design controllers with a priori chosen structure, e.g., a PI controller structure. To this end, the following definition is used.

Definition 4.1 *A set $\mathcal{K}$ is called controller structure, if there exist lower-triangular Toeplitz matrices $T_i \in \mathbb{R}^{(L-\nu)\times(L-\nu)}$, for $i = 1,\dots,d$, with at least one $T_i \neq 0_{L-\nu}$ such that*

$$\mathcal{K} = \{T \in \mathbb{R}^{(L-\nu)\times(L-\nu)} | \exists p \in \mathbb{R}^d \quad s.t. \quad T = \sum_{i=1}^{d} p_i T_i\}. \tag{4.1}$$

Since only lower-triangular basis matrices T_i are allowed in a controller structure $\mathcal{K}$, causality for a controller $K \in \mathcal{K}$ is guaranteed. In the following, when we say a controller K is of structure $\mathcal{K}$, we mean that the *Toeplitz* matrix $T(g)$ of its impulse response $\{g_k\}_{k=0}^{L-\nu-1}$ is in the set $\mathcal{K}$. An example for a controller structure $\mathcal{K}$ is the discrete PI controller structure defined by

$$T_1 = I \quad \text{and} \quad T_2 = \begin{pmatrix} 0 & 0 & \dots & 0 \\ T_s & 0 & \dots & 0 \\ \vdots & \ddots & \ddots & \vdots \\ T_s & \dots & T_s & 0 \end{pmatrix}, \tag{4.2}$$

with sampling rate T_s. Note that no specific structure needs to be imposed on the controller. This can be achieved by choosing T_i, for $i = 1,\dots,L-\nu$, as square matrices of size $L-\nu$ with ones on the $(i-1)$-th diagonal below the main diagonal, i.e., $i = 1$ represents the main diagonal. Using this structure all controllers with finite-length impulse response can be represented. Thus, if a controller is of structure $\mathcal{K}$, we can parametrize its *Toeplitz* matrix by

$$T(g(p)) = \sum_{i=1}^{d} p_i T_i,$$

which is linear in p. Hence, the matrices $M_{L-\nu}(g(p))$ in Proposition 3.2 and therefore also in Theorem 3.1 are also linear in the new controller parameters p for all channels ($r \mapsto z$, $r \mapsto e$, $r \mapsto u$) in the standard feedback loop. Given data (u,y) of the plant G, a controller structure $\mathcal{K}$ and an L-dissipativity specification, we can translate the analysis inequalitiy into a synthesis inequality in the parameters p via the following theorem.

Theorem 4.1 *Let $\mathcal{K}$ be a desired controller structure and the supply rate Π with the horizon L a desired dissipativity specification for the standard feedback loop from $r \mapsto z$. Suppose furthermore that $\{u_k,y_k\}_{k=0}^{N-1}$ is a trajectory of the plant G, where u is persistently exciting of order $L+n$. Then, for any ν with $n \leq \nu < L$, there exists a controller K of structure $\mathcal{K}$ that renders the closed loop from $r \mapsto z$ $(L-\nu)$-dissipative w.r.t. the supply rate Π if and only if the QMI in p*

$$V_L^\nu(u,y)^\top H_L(u,y)^\top J_L^{\nu\top} M_{L-\nu}(g(p))^\top \Pi_{L-\nu} M_{L-\nu}(g(p)) J_L^\nu H_L(u,y) V_L^\nu(u,y) \succcurlyeq 0, \tag{4.3}$$

where

$$M_{L-\nu}(g(p)) = \begin{pmatrix} I_{L-\nu} & T(g(p)) \\ 0_{L-\nu} & T(g(p)) \end{pmatrix},$$

has a solution $\hat{p}$ and the resulting controller K, represented by $T(g(\hat{p})) = \sum_{i=1}^d \hat{p}_i T_i$, renders the closed loop well-posed.

Proof Combining Theorem 3.1 with Definition 4.1 directly leads us to the inequality (4.3) and to the well-posedness condition and vice versa. Furthermore, it remains to show that (4.3) is a QMI in the newly introduced controller parameters p. To this purpose, we use the following abbreviation

$$\begin{aligned} N_u(u,y) &= J_L^\nu H_L(u) V_L^\nu(u,y), \\ N_y(u,y) &= J_L^\nu H_L(y) V_L^\nu(u,y) \end{aligned} \tag{4.4}$$

and define the following matrices

$$\begin{aligned} Q_0 &= -N_u(u,y)^\top Q_{L-\nu} N_u(u,y), \\ Q_i &= -N_u(u,y)^\top (Q_{L-\nu}+S_{L-\nu}) T_i N_y(u,y) - N_y(u,y)^\top T_i^\top (Q_{L-\nu}+S_{L-\nu}^\top) N_u(u,y), \\ V_{ij} &= -N_y(u,y)^\top T_i^\top (Q_{L-\nu} + S_{L-\nu} + S_{L-\nu}^\top + R_{L-\nu}) T_j N_y(u,y), \\ Q_{ij} &= \begin{cases} V_{ij}, & \text{if } i=j \\ V_{ij}+V_{ji}, & \text{if } i<j \\ 0, & \text{else} \end{cases}. \end{aligned} \tag{4.5}$$

Then, multiplying (4.3) out yields

$$Q(p) = Q_0 + \sum_{i=1}^d p_i Q_i + \sum_{i=1}^d \sum_{j=1}^d p_i p_j Q_{ij} \preccurlyeq 0,$$

which is by (1.1) a QMI in p and therefore concludes the proof. ∎

Theorem 4.1 is the natural extension of Theorem 3.1, from the analysis condition to the synthesis inequality, taking a special controller structure $\mathcal{K}$ into consideration. It allows us to design controllers by defining a dissipativity specification and solving the corresponding synthesis inequality (4.3) for the controller parameters p.

Remark 4.1 *Of course, as mentioned for Theorem 3.1, Theorem 4.1 can be stated for the other channels, $r \mapsto u$ and $r \mapsto e$, in the standard feedback loop (Figure 1.2), as well. For the channel $r \mapsto u$ the QMI matrices are*

$$
\begin{aligned}
Q_0 &= -N_u(u,y)^\top Q_{L-\nu} N_u(u,y),\\
Q_i &= -N_u(u,y)^\top Q_{L-\nu} T_i N_y(u,y) - N_u(u,y)^\top S_{L-\nu} T_i N_u(u,y)\\
&\quad - N_y(u,y)^\top T_i^\top Q_{L-\nu} N_u(u,y) - N_u(u,y)^\top T_i^\top S_{L-\nu} N_u(u,y),\\
V_{ij} &= -(\star)^\top \begin{pmatrix} T_i & 0_{L-\nu} \\ 0_{L-\nu} & T_i \end{pmatrix}^\top \begin{pmatrix} Q_{L-\nu} & S_{L-\nu} \\ S_{L-\nu}^\top & R_{L-\nu} \end{pmatrix} \begin{pmatrix} T_j & 0_{L-\nu} \\ 0_{L-\nu} & T_j \end{pmatrix} \begin{pmatrix} N_u(u,y) \\ N_y(u,y) \end{pmatrix},\\
Q_{ij} &= \begin{cases} V_{ij}, & \text{if } i = j \\ V_{ij} + V_{ji}, & \text{if } i < j \\ 0, & \text{else} \end{cases}
\end{aligned}
\tag{4.6}
$$

and for the channel $r \mapsto e$ the matrices read

$$
\begin{aligned}
Q_0 &= -N_u(u,y)^\top (Q_{L-\nu} + S_{L-\nu} + S_{L-\nu}^\top + R_{L-\nu}) N_u(u,y),\\
Q_i &= -N_u(u,y)^\top (Q_{L-\nu} + S_{L-\nu}^\top) T_i N_y(u,y) - N_y(u,y)^\top T_i^\top (Q_{L-\nu} + S_{L-\nu}) N_u(u,y),\\
V_{ij} &= -N_y(u,y)^\top T_i^\top Q_{L-\nu} T_j N_y(u,y),\\
Q_{ij} &= \begin{cases} V_{ij}, & \text{if } i = j \\ V_{ij} + V_{ji}, & \text{if } i < j \\ 0, & \text{else} \end{cases}.
\end{aligned}
\tag{4.7}
$$

Clearly, solving the synthesis QMI for a suitable controller parametrization p is in general a non-convex problem, which cannot be solved in a straightforward fashion. In Section 4.2, we discuss two approaches to solve the QMI.

4.2. Solution of the synthesis inequality

In general, a QMIFP is a non-convex problem, which makes it difficult to solve globally or even solve at all. In this section, two approaches are presented: First, if the given QMI is convex, it can be turned into an LMI, which can then be solved by LMI techniques. Secondly, a DC programming approach is presented, which can be used to obtain a solution for the general non-convex case, but gives only sufficient computational guarantees.

4.2.1. Convex case

An LMI defines a convex set in its decision variable, whereas this does not hold for a QMI in general. Convexity of a QMI allows us to reformulate it into an LMI which can then be efficiently solved via convex optimization methods, especially *Interior Point* methods. To this purpose, a general QMI of the form (1.1) can be expressed as

$$Q(\xi) = Q_0 + \hat{Q}\tilde{\Xi} + \tilde{\Xi}^\top \tilde{Q}\tilde{\Xi} \preccurlyeq 0, \tag{4.8}$$

where $\tilde{\Xi} = \xi \otimes I$, $\hat{Q} = \begin{pmatrix} Q_1 & \dots & Q_{n_q} \end{pmatrix}$ and

$$\tilde{Q} = \begin{pmatrix} Q_{11} & \dots & Q_{1n_q} \\ \vdots & \ddots & \vdots \\ Q_{n_q 1} & \dots & Q_{n_q n_q} \end{pmatrix}. \tag{4.9}$$

In this form, convexity of a QMI can be ensured by the following lemma.

Lemma 4.1 ([34, Lemma 1]) *The QMI constraint $Q(\xi) \preccurlyeq 0$ in (1.1) forms a convex set for the decision variable ξ, if the corresponding matrix $\tilde{Q}$ in (4.9) is positive semidefinite.*

This positive semidefiniteness condition on $\tilde{Q}$ allows us to state the following result, which summarizes results from [34], which are again proven in this thesis for the reasons of insight and completeness.

Lemma 4.2 ([34]) *The QMI $Q(\xi) \preccurlyeq 0$ is equivalent to the LMI*

$$\begin{pmatrix} -I & U\tilde{\Xi} \\ \tilde{\Xi}^\top U^\top & Q_0 + \hat{Q}\tilde{\Xi} \end{pmatrix} \preccurlyeq 0,$$

with $\tilde{Q} = U^\top U$, if $\tilde{Q} \succcurlyeq 0$.

Proof The assumption $\tilde{Q} \succcurlyeq 0$ allows us to factorize $\tilde{Q}$ by $\tilde{Q} = U^\top U$ with $U \in \mathbb{R}^{\bullet\times\bullet}$ by choosing, e.g., U as $U = \tilde{Q}^{\frac{1}{2}}$ [13, Theorem 7.2.7]. Therefore, we can rewrite (4.8) as

$$Q(\xi) = Q_0 + \hat{Q}\tilde{\Xi} - \tilde{\Xi}^\top U^\top (-I) U \tilde{\Xi} \preccurlyeq 0$$

and apply a *Schur Complement* (see Lemma A.1 in the Appendix) to find the equivalent semidefiniteness condition

$$\begin{pmatrix} -I & U\tilde{\Xi} \\ \tilde{\Xi}^\top U^\top & Q_0 + \hat{Q}\tilde{\Xi} \end{pmatrix} \preccurlyeq 0. \tag{4.10}$$

Since all terms in (4.10) depend affinely on $\tilde{\Xi}$, and $\tilde{\Xi}$ is linear in the decision variables ξ, (4.10) is an LMI in ξ, which concludes the proof. ■

The semidefiniteness condition on $\tilde{Q}$, for our special synthesis inequalities for all channels in the standard feedback loop with the matrices defined in (4.5), (4.6) and (4.7), translates into the condition $V_{ii} \succcurlyeq 0$, for $i = 1, \ldots, d$, because of the special structure in

$$\tilde{Q} = \begin{pmatrix} V_{11} & (V_{12} + V_{21}) & \ldots & (V_{1d} + V_{d1}) \\ 0 & V_{22} & \ddots & \vdots \\ \vdots & \ddots & \ddots & (V_{(d-1)d} + V_{d(d-1)}) \\ 0 & \ldots & 0 & V_{dd} \end{pmatrix}$$

and the eigenvalues of a block-triangular matrix are the combined eigenvalues of its diagonal blocks.

If we look at the matrices

$$V_{ii} = -N_y(u,y)^\top T_i^\top (Q_{L-\nu} + S_{L-\nu} + S_{L-\nu}^\top + R_{L-\nu}) T_i N_y(u,y)$$

from (4.5) for the channel $r \mapsto z$, $V_{ii} \succcurlyeq 0$, for $i = 1, \ldots, d$, can be ensured by

$$(Q_{L-\nu} + S_{L-\nu} + S_{L-\nu}^\top + R_{L-\nu}) \preccurlyeq 0. \tag{4.11}$$

Of course this condition is not necessary for $V_{ii} \succcurlyeq 0$, but yields a nice condition in terms of the supply rate, under which the synthesis inequality (4.3), for the channel $r \mapsto z$, can be turned into an LMI.

Remark 4.2 *A sufficient condition in terms of the supply rate Π for the convexity of the synthesis inequality (4.3) for the channel $r \mapsto e$, and therefore the ability of rewriting the inequality into an LMI, is given by*

$$Q_{L-\nu} \preccurlyeq 0. \tag{4.12}$$

For the channel $r \mapsto u$, it would not be useful to state a condition in terms of the supply rate, since the condition

$$\begin{pmatrix} Q_{L-\nu} & S_{L-\nu} \\ S_{L-\nu}^\top & R_{L-\nu} \end{pmatrix} \preccurlyeq 0 \tag{4.13}$$

contradicts the dissipativity conditions for L-dissipativity in Definition 2.4 itself.

In conclusion, (4.11) is a condition on the supply rate matrices for the given dissipativity specification to translate the corresponding synthesis inequality (4.3) into an LMI via Lemma 4.2 and apply LMI techniques to yield a satisfying controller parametrization p. The great advantage is that we can solve the inequality globally and therefore can guarantee infeasibility/feasibility through the available numerical solvers, e.g., [1]. Unfortunately, the shown conditions for the supply rate, can be quite restrictive in the selection of a dissipativity specification. Therefore, in Section 4.2.2, an algorithm for the general non-convex case is presented, which at least is able to provide a feasible solution in a local manner, if the algorithm is initialized in the neighborhood of a solution.

4.2.2. General case

As mentioned above the reformulation of the synthesis inequality (4.3) into an LMI is only possible under certain restrictive semidefiniteness conditions on the supply rate. Therefore, it is necessary to develop further tools for solving (4.3) in the general non-convex case for a controller parametrization p in the given controller structure $\mathcal{K}$. To this end, a DC programming approach is employed to find a feasible solution for a general QMI and therefore also the synthesis inequality. A general DC program has the form

$$\inf\{g(\xi) - h(\xi) : \xi \in \mathbb{R}^{n_{dc}}\}, \tag{4.14}$$

where g, h are convex. The idea of DC programming goes back to 1985. There are several publications since then, including general theory (existence of a solution, convergence of difference of convex functions algorithm (DCA)),

singled out [28], and several applications to real world problems and specific non-convex problems. A recent survey on the developments of DC programming for both, theory and algorithmic tools, is available in [18]. The main concept of the DCA is the approximation of a non-convex DC program by iteratively solving convex ones. Therefore, two sequences $\{\xi_k\}$ and $\{\psi_k\}$ are constructed, which guarantee that the resulting sequences $\{g(\xi_k) - h(\xi_k)\}$ and $\{h^*(\xi_k) - g^*(\xi_k)\}$ are decreasing. Given an initial starting point $\xi_0 \in \mathbb{R}^{n_{dc}}$ for the DC program, at each iteration k, calculate

1.
$$\psi_k \in \partial h(\xi_k) \tag{4.15}$$

2.
$$\xi_{k+1} \in \partial g^*(\psi_k) \tag{4.16}$$

for the general DCA. Note that $\partial g^*(\psi_k)$ can be determined by

$$\partial g^*(\psi_k) = \underset{\xi \in \mathbb{R}^{n_{dc}}}{\arg\min}\, g(\xi) - [h(\xi_k) + \langle \xi - \xi_k, \psi_k \rangle] \quad (P_k)$$

and $\partial h(\xi_k)$ can be obtained from

$$\partial h(\xi_k) = \underset{\psi \in \mathbb{R}^{n_{dc}}}{\arg\min}\, h^*(\psi) - [g^*(\psi_{k-1}) + \langle \xi_k, \psi - \psi_{k-1} \rangle] \quad (D_k).$$

(P_k) is a convex program in ξ as well as (D_k) is convex in ψ. Therefore, for generating the sequences $\{\xi_k\}$ and $\{\psi_k\}$ one has to iteratively solve convex programs, by using the components g, h of the DC (4.14) separately. Convergence of DCA is always guaranteed independently of the initial starting point ξ_0, however there are no guarantees that the limit value of this sequence results in a global solution of the optimization problem. More explicitly, depending on the choice of ξ_0, DCA can converge to a non-global solution and ξ_0 can affect the number of necessary iterations. The complete convergence theorem and the proof of this proposed generating scheme can be found in [28, Theorem 3]. In this thesis, no further details about the general theory of DC programming are given, rather than applying the concept of DC programming to the QMIFP, which is extensively studied in [26]. For more details about DC programming in general, we refer to [28].

In order to apply the DC programming approach to the controller synthesis problem, a general QMIFP of the form (1.1) has to be rewritten into a DC

program of the form (4.14). Therefore, a QMI (1.1) in ξ can be rewritten into

$$Q(\xi,W) = Q_0 + \sum_{i=1}^{n_q} \xi_i Q_i + \sum_{i=1}^{n_q}\sum_{j=1}^{n_q} w_{ij} Q_{ij}, \tag{4.17}$$

where

$$(\xi,W) \in \{(\xi,W) \in \mathbb{R}^{n_q} \times \mathbb{S}^{n_q} : W = \xi\xi^\top\}$$

by replacing the bilinear/quadratic terms $\xi_i\xi_j$ with new variables w_{ij}. $Q(\xi,W)$ in (4.17) depends now affinely on its variables ξ and W and is therefore a convex constraint. However, the additional equality constraint $W = \xi\xi^\top$ does destroy convexity. This additional constraint can also be expressed as follows.

Lemma 4.3 ([32, Lemma 5]) *Let $W \in \mathbb{S}^{n_q}$ and $\xi \in \mathbb{R}^{n_q}$. Then, $W = (w_{ij}) = \xi\xi^\top$ if and only if*

$$\begin{pmatrix} W & \xi \\ \xi^\top & 1 \end{pmatrix} \succcurlyeq 0 \quad \textit{and} \tag{4.18}$$

$$\operatorname{trace}(W - \xi\xi^\top) \leq 0. \tag{4.19}$$

Proof First, notice that (4.18) is equivalent to $\tilde{W} = W - \xi\xi^\top \succcurlyeq 0$ by applying the Schur Complement from Lemma A.1 in the Appendix.

if: From (4.18), i.e., from $\tilde{W}$, and the fact that positive semidefinite matrices have non-negative entries on its diagonal, we infer $w_{ii} - \xi_i^2 \geq 0$ for $i = 1,\ldots,n_q$. Since (4.19) is equivalent to

$$\operatorname{trace}(W) - \operatorname{trace}(\xi\xi^\top) = \sum_{i=1}^{n_q} w_{ii} - \sum_{i=1}^{n_q} \xi_i^2 = \sum_{i=1}^{n_q} w_{ii} - \xi_i^2 \leq 0,$$

it follows that $w_{ii} - \xi_i^2 = 0$ for $i = 1,\ldots,n_q$. Therefore, $\operatorname{trace}(\tilde{W}) = 0$, and we conclude by Lemma A.2 from the Appendix that $\tilde{W} = 0$, and hence $W = \xi\xi^\top$.

Only if: Using $W = \xi\xi^\top$, one gets $\tilde{W} = W - \xi\xi^\top = 0 \succcurlyeq 0$ and $\operatorname{trace}(W - \xi\xi^\top) = \operatorname{trace}(0_{n_q \times n_q}) = 0$. Therefore, (4.18) and (4.19) are satisfied. ■

The proof of Lemma 4.3 is included since it provides necessary information for the upcoming results. Using this lemma, a QMIFP can be stated as done in the following result originally proven in [26]. However, we give a more detailed and structured version of the proof in [26] for a better understanding of the subject.

Lemma 4.4 ([26, Theorem 1]) *The QMI (1.1) is feasible if and only if there exists a point $(\xi,W) \in \mathcal{C}$, where*

$$\mathcal{C} = \{(\xi,W) \in \mathbb{R}^{n_q} \times \mathbb{S}^{n_q} | Q_0 + \sum_{i=1}^{n_q} \xi_i Q_i + \sum_{i=1}^{n_q}\sum_{j=1}^{n_q} w_{ij} Q_{ij} \preccurlyeq 0, \begin{pmatrix} W & \xi \\ \xi^\top & 1 \end{pmatrix} \succcurlyeq 0\},$$

and

$$\operatorname{trace}(W) - \sum_{i=1}^{n_q} \xi_i^2 = 0.$$

Proof if: If there exists $(\xi,W) \in \mathcal{C}$ with $\operatorname{trace}(W) - \sum_{i=1}^{n_q} \xi_i^2 = 0$, we can use Lemma 4.3 to infer that $W = \xi\xi^\top$. Since (ξ,W) also satisfies

$$Q(\xi,W) = Q_0 + \sum_{i=1}^{n_q} \xi_i Q_i + \sum_{i=1}^{n_q}\sum_{j=1}^{n_q} w_{ij} Q_{ij} \preccurlyeq 0,$$

we conclude with the dependency in (4.17) that

$$Q(\xi) = Q_0 + \sum_{i=1}^{n_q} \xi_i Q_i + \sum_{i=1}^{n_q}\sum_{j=1}^{n_q} \xi_i\xi_j Q_{ij} \preccurlyeq 0.$$

Only if: Suppose $\xi \in \mathbb{R}^{n_q}$ satisfies the QMI (1.1), more explicitly

$$Q(\xi) = Q_0 + \sum_{i=1}^{n_q} \xi_i Q_i + \sum_{i=1}^{n_q}\sum_{j=1}^{n_q} \xi_i\xi_j Q_{ij} \preccurlyeq 0.$$

Then, we can choose $W = \xi\xi^\top \in \mathbb{S}^{n_q}$. Again using the dependency (4.17) and Lemma 4.3, we infer that $(\xi,W) \in \mathcal{C}$ and $\operatorname{trace}(W) - \sum_{i=1}^{n_q} \xi_i^2 \leq 0$. Moreover, as seen in the proof of Lemma 4.3, $\operatorname{trace}(W) - \sum_{i=1}^{n_q} \xi_i^2 = 0$, which concludes the proof. ∎

Employing Lemma 4.4, feasibility of the QMI (1.1) can be checked by the

following concave minimization problem

$$\begin{aligned} \min_{\xi,W} \quad & \operatorname{trace}(W) - \sum_{i=1}^{n_q} \xi_i^2 \\ \text{s.t.} \quad & Q(\xi,W) = Q_0 + \sum_{i=1}^{n_q} \xi_i Q_i + \sum_{i=1}^{n_q}\sum_{j=1}^{n_q} w_{ij} Q_{ij} \preccurlyeq 0, \\ & \begin{pmatrix} W & \xi \\ \xi^\top & 1 \end{pmatrix} \succcurlyeq 0, \\ & (\xi,W) \in \mathbb{R}^{n_q} \times \mathbb{S}^{n_q}. \end{aligned} \tag{4.20}$$

The QMI is feasible if and only if the corresponding optimal cost of (4.20) is zero. The last step towards the DC formulation (4.14) is to define $g(\xi,W)$ as the indicator function $i_{\mathcal{C}}(\xi,W)$ for the convex set $\mathcal{C}$ from Lemma 4.4 and $h(\xi,W) = \sum_{i=1}^{n_q} \xi_i^2 - w_{ii}$, which is also convex. Hence the minimization problem in (4.20) is equivalent to

$$\min f(\xi,W) = \min g(\xi,W) - h(\xi,W)$$

a minimization of a difference of convex functions.

Now we are able to apply the general DCA iteration ((4.15),(4.16)) and if the solution $(\tilde{\xi},\tilde{W})$ renders the cost function $f(\tilde{\xi},\tilde{W}) = 0$, then $\tilde{\xi}$ is a solution to the corresponding QMI. The function $h(\xi,W)$ is differentiable and therefore the subdifferential $\partial h(\xi_k,W_k)$ at (ξ_k,W_k) only contains $\nabla h(\xi_k,W_k)$, which can be computed explicitly. Hence, the dual variables of the iteration satisfy $(\psi_k,Z_k) \in \partial h(\xi_k,W_k) = \{(2\xi_k, -I_{n_q})\}$. For the second step (4.16) of the DCA iteration, following program has to be solved

$$\operatorname*{arg\,min}_{(\xi,W)\in\mathbb{R}^{n_q}\times\mathbb{S}^{n_q}} g(\xi,W) - [h(\xi_k,W_k) + \langle \xi - \xi_k, \psi_k\rangle + \langle W - W_k, Z_k\rangle],$$

which can be reduced to

$$
\begin{aligned}
&\underset{(\xi,W)\in\mathbb{R}^{n_q}\times\mathbb{S}^{n_q}}{\arg\min} \quad g(\xi,W)-[h(\xi_k,W_k)+\langle\xi-\xi_k,\psi_k\rangle+\langle W-W_k,Z_k\rangle]\\
=&\underset{(\xi,W)\in\mathbb{R}^{n_q}\times\mathbb{S}^{n_q}}{\arg\min} \quad i_{\mathcal{C}}(\xi,W)-[\sum_{i=1}^{n_q}\xi_{k,i}^2-w_{k,ii}+\langle\xi,\psi_k\rangle-\langle\xi_k,\psi_k\rangle+\langle W,Z_k\rangle-\langle W_k,Z_k\rangle]\\
=&\underset{(\xi,W)\in\mathcal{C}}{\arg\min} \quad -\langle\xi_k,\xi_k\rangle+\mathrm{trace}(W_k)-\langle\xi,2\xi_k\rangle+\langle\xi_k,2\xi_k\rangle-\langle W,-I_{n_q}\rangle+\langle W_k,-I_{n_q}\rangle\\
=&\underset{(\xi,W)\in\mathcal{C}}{\arg\min} \quad \langle\xi_k,\xi_k\rangle-\langle\xi,2\xi_k\rangle+\mathrm{trace}(W)\\
=&\underset{(\xi,W)\in\mathcal{C}}{\arg\min} \quad \mathrm{trace}(W)-\langle\xi,2\xi_k\rangle.
\end{aligned}
$$

Hence, the sequences ξ_k, W_k can be generated by solving

$$
(\xi_{k+1},W_{k+1}) \in \underset{(\xi,W)\in\mathcal{C}}{\arg\min} \quad \mathrm{trace}(W)-\langle\xi,2\xi_k\rangle \tag{4.21}
$$

iteratively, without using the dual variables (ψ,Z). Note that the program in (4.21) involves the minimization of a linear objective function over the convex set $\mathcal{C}$, hence is a linear semidefinite program or otherwise known as LMI optimization problem. As mentioned for the convex case in Section 4.2.1, this can be efficiently solved by *Interior Point* algorithms. In conclusion, the overall algorithm by [26] for finding a feasible solution of a QMI can be stated (see Algorithm 4.1). Algorithm 4.1 provides a possibility to find a feasible solution to a general non-convex QMI and is very easy to implement in *Matlab* with the tool from [19] and additional LMI solvers like [1]. The solution depends on the starting value since, as mentioned for the general DCA, the DCA converges to a local minimum of its objective function. In our case, if the objective function at the found local minimum is non zero, then the local minimum is no solution to the QMI. Nevertheless, there could be another local minimum where the objective function is indeed zero and therefore the QMI has a solution. Only if the global minimum renders the objective function non zero, the QMI is infeasible. Namely, if Algorithm 4.1 returns no feasible solution, we cannot conclude that the QMI is infeasible. To overcome this issue, one can run Algorithm 4.1 over a grid of starting points ξ_0 or add other global solvers, e.g., *Branch & Bound*, around Algorithm 4.1 to ensure globality of the obtained overall solution.

Algorithm 4.1 DCA for QMIFP from [26]

1: Given:
- QMI $Q(\xi) \preccurlyeq 0$
- Starting point ξ_0
- Stopping parameters $\epsilon_1 > 0$, $\epsilon_2 > 0$

2: Initialize: $W_0 = \xi_0 \xi_0^\top$ and $k = 0$.
3: Set $f(\xi, W) = \operatorname{trace}(W) - \sum_{i=1}^{n_q} \xi_i^2$.
4: **while** True **do**
5: Solve
6:

$$
\begin{aligned}
(\xi_{k+1}, W_{k+1}) \in \arg\min \quad & \operatorname{trace}(W) - \langle \xi, 2\xi_k \rangle \\
\text{s.t.} \quad & Q_0 + \sum_{i=1}^{n_q} \xi_i Q_i + \sum_{i=1}^{n_q} \sum_{j=1}^{n_q} w_{ij} Q_{ij} \preccurlyeq 0, \\
& \begin{pmatrix} W & \xi \\ \xi^\top & 1 \end{pmatrix} \succcurlyeq 0, \\
& (\xi, W) \in \mathbb{R}^{n_q} \times \mathbb{S}^{n_q}.
\end{aligned}
$$

7: **if** $f(\xi_k, W_k) \leq \epsilon_1$ **then**
8: **return** ξ_{k+1} as feasible solution of the QMI $Q(\xi) \preccurlyeq 0$.
9: **else if** $|f(\xi_{k+1}, W_{k+1}) - f(\xi_k, W_k)| \leq \epsilon_2 |f(\xi_k, W_k)|$ **then**
10: **return** No feasible solution found.
11: **else**
12: Set $k = k + 1$.
13: **end if**
14: **end while**

Remark 4.3 *Multiple QMIs in one variable can be incorporated to one big QMI by diagonal augmentation. Given multiple QMIs $Q_i(\xi) \preccurlyeq 0$, for $i = 1, \ldots, h$, finding a feasible point ξ for all QMIs is equivalent to finding a feasible point ξ for the QMI*

$$
Q(\xi) = \begin{pmatrix} Q_1(\xi) & & \\ & \ddots & \\ & & Q_h(\xi) \end{pmatrix} \preccurlyeq 0 \tag{4.22}
$$

In conclusion, Algorithm 4.1 can also be used to solve multiple QMIs simultaneously.

Remark 4.4 *Additional convex constraints on the variables ξ, e.g., LMI constraints, can be easily added to the DCA for QMI by constraining the set $\mathcal{C}$ further. They do not have to be formulated as a QMI without quadratic terms and added to the original QMI by diagonal augmentation, rather then explicitly added to the constraints in the optimization problem in Algorithm 4.1.*

Since we are now able to find a solution to a QMI for both, the convex and non-convex case (only sufficient computational guarantees), we can apply these tools to solve the synthesis inequality (4.3) for controller design. This is shown numerically for an example system in Section 4.4, after a summary of the data-driven design procedure in Section 4.3.1 and useful specifications (Section 4.3.2) for controller design in the standard feedback loop.

4.3. Controller design

This section summarizes the whole data-driven design procedure via finite-horizon dissipativity, as well as state some dissipativity specifications, e.g., mixed sensitivity design [17], and additional constraints on the controller parameters, which can be useful for the standard feedback loop.

4.3.1. Design procedure

In this subsection, the overall controller design process following from the presented results is stated. As already mentioned in Remark 4.3, multiple QMIs can be collected into one big QMI by diagonal augmentation. Applying this to our design process gives us the opportunity to not only design controller constrained by one single dissipativity specification in the standard feedback loop, but rather impose multiple dissipativity constraints on all different input-output channels in form of multiple synthesis inequalities $Q_i(p) \preccurlyeq 0$ for $i = 1, \dots, h$. More precisely, we are able to perform multi-objective structured controller design via a QMIFP. In comparison, in the model-based setting, structured controller design, as well as multi-objective design via LMI techniques [30], is in general difficult, because of the necessary convexifying controller parameter transformation. However, a direct comparison of both methods is difficult since we allow for QMIs in the data-driven synthesis approach, which introduce aforementioned limitations to

the LMI based solutions. Another great feature of the presented framework is that additional constraints on the controller parameters p can be added on top of the dissipativity specifications for the closed loop. In Definition 4.1, the definition of the controller structure, we did not impose any constraints on p, but we can directly introduce them as additional QMI or LMI constraints

$$Q_c(p) \preccurlyeq 0.$$

In summary, the overall synthesis inequality

$$Q(p) = \begin{pmatrix} Q_1(p) & & & \\ & \ddots & & \\ & & Q_h(p) & \\ & & & Q_c(p) \end{pmatrix} \preccurlyeq 0 \tag{4.23}$$

in the controller parameter p gathers all dissipativity specifications (from Theorem 4.1) for the standard feedback loop as well as the additional controller parameter constraints. To summarize the whole design procedure, Algorithm 4.2 can be used to perform data-driven multiobjective structured controller design for the standard feedback loop via finite horizon dissipativity.

4.3.2. Specifications

After stating the overall design procedure, some more intuiton on how the framework can be used is given. Namely, some exemplary dissipativity specifications as well as exemplary controller parameter constraints are introduced. Multiobjective design gives us the opportunity to perform mixed sensitivity design [17], where the transfer functions from $r \mapsto e$ and $r \mapsto u$ are shaped through the introduction of additional filters W_e and W_u with impulse responses g_{W_e} and g_{W_u}. More specifically, the standard feedback loop (Figure 1.2) is artificially extended to the feedback loop in Figure 4.1. These filters are added to the outputs of the channels and the input-output behavior of these new outputs can be described by

$$\begin{pmatrix} r \\ k_W \end{pmatrix} = \begin{pmatrix} I_{L-\nu} & 0_{L-\nu} \\ 0_{L-\nu} & T(g_{W_k}) \end{pmatrix} M_{L-\nu}(g(p)) J_L^\nu H_L(u,y) V_L^\nu(u,y) \beta,$$

for $k = e, u$, via an extension of Proposition 3.2. If now, an $\mathcal{L}_2$-gain specification with $\gamma = 1$ (see (2.2)) from the reference r to the output of the filters is

Algorithm 4.2 Data-driven controller design via finite-horizon dissipativity

1: Given:
- Upper bound ν on the state dimension of the unknown plant G
- Closed-loop dissipativity specifications in terms of supply rates Π_i and different horizons $L_i - \nu$ for the channel $r \mapsto k_i \in \{z,e,u\}$ for $i = 1,\dots,h$
- Controller structure $\mathcal{K}$
- Controller parameter constraints $Q_c(p) \preccurlyeq 0$

2: Collect input-output trajectory of the plant G with persistently exciting input of order $\max_i L_i + \nu$.
3: Derive all dissipativity synthesis inequalities $Q_i(p) \preccurlyeq 0$ for $i = 1,\dots,h$ by Theorem 4.1 for the corresponding channel k_i.
4: Formulate overall synthesis inequality $Q(p) \preccurlyeq 0$ via (4.23).
5: **if** $Q(p)$ is convex **then**
6: Use Lemma 4.2 to rewrite $Q(p) \preccurlyeq 0$ into an LMI and use LMI techniques to solve for a satisfying controller parametrization p.
7: **else**
8: Use Algorithm 4.1 to find a suitable controller parametrization p.
9: **end if**
10: Apply the controller $u = T(g(p))e$.

imposed, the transfer functions of $r \mapsto u$ and $r \mapsto e$ are then shaped in the sense that (for a sufficiently long horizon $L - \nu$) the magnitude response of the inverses of these filters is an upper bound for the magnitude response of these sensitivity transfer functions. Generally speaking, we can perform loopshaping of the closed loop by introducing these filters and impose $\mathcal{L}_2$-gain specifications on the newly created channels (reference to output of the filters). Therefore, the creation of dissipativity specifications for mixed sensitivity design would be as follows:

1. Design filters W_e and W_u such that the magnitude response of the inverses of these filters meet the closed-loop requirements.

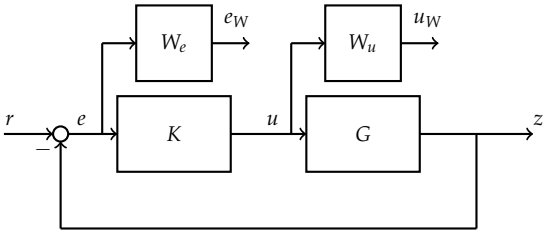

Figure 4.1.: Feedback loop for mixed sensitivity design.

2. Replace the stacked supply rate $\Pi_{L-\nu}$ in (4.3) by

$$\tilde{\Pi}_{L-\nu,k} = (\star)^\top \begin{pmatrix} I_{L-\nu} & 0_{L-\nu} \\ 0_{L-\nu} & -I_{L-\nu} \end{pmatrix} \begin{pmatrix} I_{L-\nu} & 0_{L-\nu} \\ 0_{L-\nu} & T(g_{W_k}) \end{pmatrix} \tag{4.24}$$

for $k = e,u$ for the channels $r \mapsto e$ and $r \mapsto u$.

Examples for closed-loop requirements for $r \mapsto e$ are, low gain at small frequencies, high gain at high frequencies for good tracking and disturbance attenuation. For $r \mapsto u$ one can choose, e.g., a constant magnitude response to keep the control energy small. We have now presented one possibility to use finite-horizon dissipativity for controller design as a general idea how the framework can be used. For the theoretical results in this thesis, noise-free measurements were assumed, which is never the case in practice. A simple remedy, proposed in [29], for handling noisy data for a given dissipativity synthesis inequality $Q(p) \preccurlyeq 0$ is to use the relaxation

$$Q(p) \preccurlyeq \delta I, \tag{4.25}$$

where $\delta > 0$ is a parameter depending on the size of the noise. Of course, this relaxation is without desirable guarantees, but can be used for all types of uncertainties.

In Section 4.3.1, it was mentioned that additional constraints on the controller parameters p can be incorporated into the framework. For example, if one wants to impose a box constraint

$$p \in \{\xi \in \mathbb{R}^d : \underline{p}_i \leq \xi_i \leq \overline{p}_i, i = 1, \ldots, d\}$$

by adding

$$Q_c(p) = \begin{pmatrix} \underline{p}_1 & 0 & & & \\ 0 & -\overline{p}_1 & & & \\ & & \ddots & & \\ & & & \underline{p}_d & 0 \\ & & & 0 & -\overline{p}_d \end{pmatrix} + \begin{pmatrix} -p_1 & 0 & & & \\ 0 & p_1 & & & \\ & & \ddots & & \\ & & & -p_d & 0 \\ & & & 0 & p_d \end{pmatrix} \preccurlyeq 0$$

to the overall synthesis inequalitiy. This gives the opportunity to restrict the parameter values to a certain range, which can be based on prior knowledge of the plant or anything else. Another way to use the additional constraints for controller design is to bound the matrix norm of the *Toeplitz* matrix $T(g(p))$ to limit the control energy or even achieve finite-horizon input-output stability by using similar arguments as in the small gain criterion. More precisely, one can calculate the finite-horizon $\mathcal{L}_2$-gain γ of the plant G via Theorem 2.2 and impose a strict upper bound of $\frac{1}{\gamma}$ to the norm of $T(g(p))$ to obtain a finite-horizon $\mathcal{L}_2$-gain $\gamma_{cl} < 1$ of the closed loop. The condition on the controller can be implemented by adding the convex constraint $T(g(p))^\top T(g(p)) \prec 0$ to the overall inequality. For a large enough horizon $L - \nu$, this implies that the (infinite-horizon) closed-loop $\mathcal{L}_2$-gain is bounded by $\frac{1}{\gamma_{cl}}$, compare [16].

After summarizing the design procedure, as well as stating some exemplary design specifications to give some intuition about the presented framework, it is applied to an example system in Section 4.4.

4.4. Numerical example

In this section, the presented results for data-driven controller design, especially Algorithm 4.2, are applied to an example control problem. The goal is to design a controller K in the standard feedback loop for an unknown plant G such that the closed loop is able to perform reference tracking and disturbance attenuation. The whole process is performed numerically in *Matlab*. For the "unknown" plant G, a two-tank system is used, as shown in Figure 4.2, where the input is the voltage u applied to the water pump which generates a flow $v = ku$ towards the first tank with level h_1. The output of the first tank is connected to the second tank with level h_2, which is measurable and represents the output $y = h_2$ of the plant. The output of the second tank is connected to a big water reservoir, to which the pump has

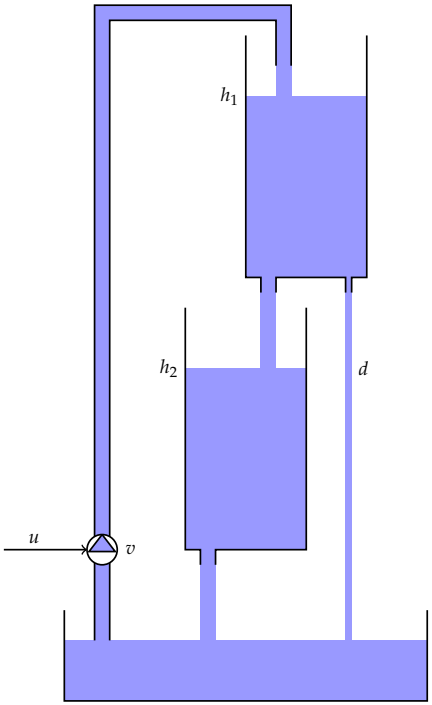

Figure 4.2.: Two tank system.

also access to. There is an additional output at the first tank which cannot be measured and can be viewed as a disturbance d. The nonlinear system without disturbance can be modeled as

$$\dot{h}_1(t) = -\frac{a_1}{A_1}\sqrt{2gh_1(t)} + \frac{k}{A_1}u(t),$$
$$\dot{h}_2(t) = -\frac{a_2}{A_2}\sqrt{2gh_2(t)} + \frac{a_1}{A_2}\sqrt{2gh_1(t)},$$

where h_1 and h_2 are the states, and therefore we have $n = 2$ for the plant. The model parameters are listed in Table 4.1. Since this system is nonlinear

Parameter	Value	Unit	Description
A_1	15.518	cm^2	Cross-section tank 1
A_2	15.518	cm^2	Cross-section tank 2
a_1	0.178	cm^2	Cross-section outflow tank 1
a_2	0.178	cm^2	Cross-section outflow tank 2
g	981	$\frac{\mathrm{cm}}{\mathrm{s}^2}$	Gravitational acceleration constant
k	4.3	$\frac{\mathrm{cm}^3}{V\mathrm{s}^2}$	Water pump constant

Table 4.1.: Two-tank model parameters.

and the framework in this thesis would not be applicable, we consider the system around a stationary point $h_1 = h_{1,0} = 15$, $h_2 = h_{2,0} = 15$, with the corresponding input $u = u_0 = 7.1054$, to at least reduce the nonlinearity. In addition, our plant is a continuous-time system, which needs additional discretiziation blocks to meet the requirements of the controller design framework. To this purpose, our controller K is connected to the plant G as shown in Figure 4.3, where S is a sampling element and H a zero-order hold

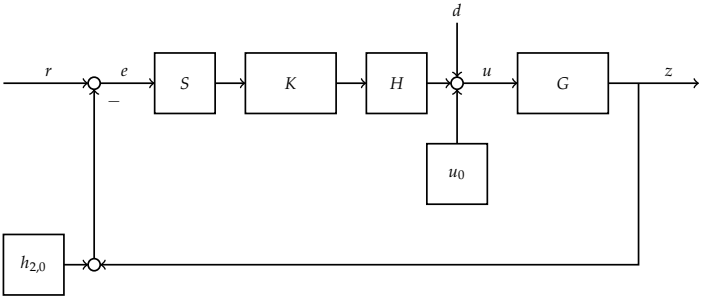

Figure 4.3.: Feedback loop for the two tank system.

element converting the continuous-time signal in a DT signal with sampling rate $T_s = 1.5$ and vice versa. The disturbance d, the additional output in tank 1, is modeled by an input disturbance to the plant. To achieve good tracking and disturbance attenuation, we follow Algorithm 4.2:

1. Collect all necessary algorithm information: ν can be set as $\nu = n = 2$,

since the state dimension is known to us. Further, the mixed sensitivity design, explained in Section 4.3.2, is used for the dissipativity specifications. To this purpose, the filters W_e and W_u with magnitude responses

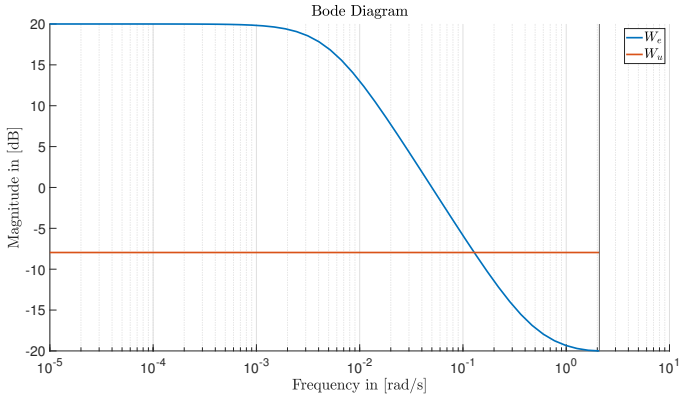

Figure 4.4.: Magnitude response of the filters from mixed sensitivity design.

as shown in Figure 4.4 are used and horizons $L_1 = L_2 = L = 175$ are chosen. The resulting supply rates for mixed sensitivity design can be seen in (4.24). As controller structure $\mathcal{K}$, the PI structure with sampling rate $T_s = 1.5$ and basis matrices as defined in (4.2) are used. Since we are dealing with a nonlinear plant, the relaxation (4.25) with $\delta = 0.5$ is used. No further constraints on the controller parameters p are imposed.

2. An input-output trajectory (u,y) of the plant G with persistently exciting input u of order $L+n$ in open loop is collected. Therefore, a trajectory (u',y') of length $N = 524$ is generated by simulation of the continuous-time model with a uniform random input signal u' in the range of $-2+u_0$ and $2+u_0$ in *Matlab* and discretization of that simulated trajectory to match the sampling rate of $T_s = 1.5$. For the simulation, initial values of $h_1(0) = h_{1,0}$ and $h_2(0) = h_{2,0}$ for the model are used. As explained above, since the model is nonlinear, the trajectory (u',y') is shifted by u_0 and $h_{2,0}$ to reduce the nonlinearity. Therefore, we obtain the DT trajectory $(u,y) = (u',y') - (u_0, h_{2,0})$ (with

slight abuse of notation) of length N with persistently exciting input u of order $L + n$.

3. Since we have two dissipativity specifications from the mixed sensitivity design, we end up with two synthesis inequalities $Q_1(p) \preccurlyeq 0$ and $Q_2(p) \preccurlyeq 0$ using Theorem 4.1. The therefore needed matrices can be constructed from the collected trajectory (u,y), the controller structure $\mathcal{K}$ and the mixed sensitivity supply rates.

4. Putting both synthesis inequalities together by diagonal augmentation the overall synthesis inequality reads

$$Q(p) = \begin{pmatrix} Q_1(p) & 0 \\ 0 & Q_2(p) \end{pmatrix} \preccurlyeq 0.$$

5. $Q(p)$ is not convex, hence we cannot use LMI techniques directly. Nevertheless, we can apply the DCA for QMIs, Algorithm 4.1, to find a feasible controller parametrization p. To further increase the chance of finding a solution, Algorithm 4.1 is initialized over the grid $\{-5,-4,-3,\ldots,3,4,5\} \times \{-1,-0.9,-0.8,\ldots,0.8,0.9,1\}$ and solved simultaneously using the *Parallel Computing Toolbox* in *Matlab*. The obtained solution is

$$p = \begin{pmatrix} 1.0278 \\ 0.0220 \end{pmatrix},$$

where p_1 is the proportional part and p_2 the integral part of the PI controller.

6. We apply the input $u = T(g(p))e$, which can be done by implementing the controller K by using the transfer function

$$K(z) = p_1 + \frac{p_2 Ts}{z-1}$$

of an *Euler* forward discretized PI controller.

The performance of the controller for reference tracking, as well as for disturbance attenuation can be seen in Figure 4.5. The reference signal in Figure 4.5 was chosen to be a step signal of magnitude 2 and the additional output of the first tank (disturbance d) was opened after 250s, which can

in our setting be done by using the following continuous-time disturbance signal

$$d(t) = \begin{cases} 0, & \text{for } 0 \leq t < 250 \\ -0.5, & \text{for } t \geq 250 \end{cases}.$$

The tank model was excited at the stationary point, i.e., the initial states were set to $h_1(0) = h_{1,0}$ and $h_2(0) = h_{2,0}$. It can be seen in Figure 4.5 that the reference is well tracked without steady state error. Recall from

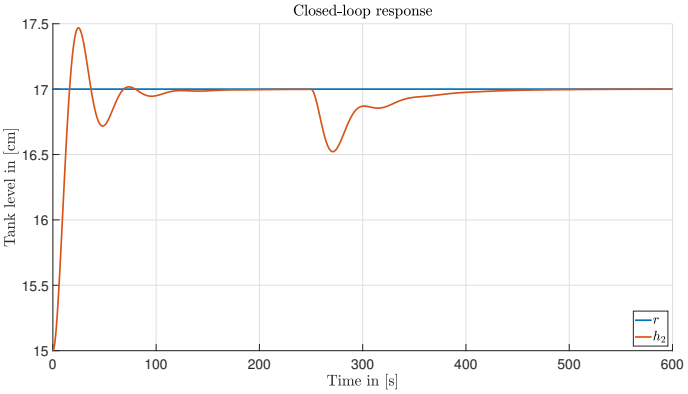

Figure 4.5.: Closed-loop response with designed controller K.

Figure 4.3 that the reference is relative to the stationary point. After opening the disturbance output, the tank level h_2 drops slightly and immediately recovers to its setpoint, and therefore the controller achieves disturbance attenuation. In conclusion, the dissipativity specifications from mixed sensitivity design with a large enough horizon, a PI controller structure and the application of Algorithm 4.2 for data-driven controller design were used to yield a controller that satisfies the given goals of good reference tracking and disturbance attenuation.

To further give an intuition on how noise affects the synthesis inequality $Q(p) \preccurlyeq 0$, Figure 4.6 compares the maximum eigenvalue of $Q(p)$ to the noise level θ. In more detail, as done in Section 3.6.1, we analyze the behavior when the output of the plant data (u,y) is affected by noise. We can only measure the noisy output $\tilde{y} = y + 2\theta(\text{rand}(N,1) - 0.5ones(N,1))$. The effect of this noisy measurement on the maximum eigenvalue of $Q(p)$, with p

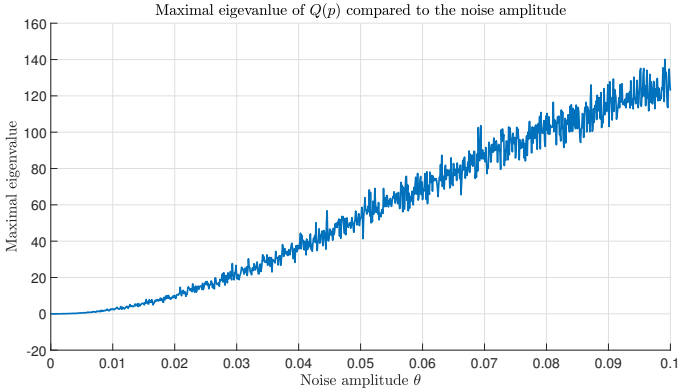

Figure 4.6.: Maximum eigenvalue of $Q(p)$ with noisy data.

as calculated in the controller design process, can be seen in Figure 4.6. For very small $\theta < 0.005$, there is barely any change visible, but after that the eigenvalue is increasing significantly rendering the synthesis inequality infeasible. For $\theta = 0.02$, for example, the relaxation parameter δ has to be increased to $\delta = 10$ for $Q(p)$ to satisfy the inequality. If increasing δ too much, we allow other controllers to be feasible, which have bad performance but do satisfy the given inequality due to the relaxation. For example if δ is too big, $p = 0$ is always a solution, which of course is not a desirable controller. In conclusion, even for small noise levels the eigenvalues can change significantly and the presented relaxation works only for relatively small noise levels.

Unfortunately, this is a drawback of the presented framework, since it does not account for noisy measurements but it can serve as a starting point for further extensions, which are better applicable to real systems. However, the framework can manage the nonlinearity of the model, which can also be seen as noise since for small deviations $\Delta h = h - h_0$ and $\Delta u = u - u_0$ around the stationary point (h_0,u_0) of a nonlinear model of the form $\dot{h} = f(h,u)$, the linear terms in

$$\Delta\dot{h} = \underbrace{\frac{\partial f}{\partial h}\Big|_{h_0,u_0}}_{\tilde{A}} \Delta h + \underbrace{\frac{\partial f}{\partial u}\Big|_{h_0,u_0}}_{\tilde{B}} \Delta u + \mathcal{O}(\Delta h^2) + \mathcal{O}(\Delta u^2)$$

dominate over the nonlinear parts. Hence, the terms of higher order can be modeled as process noise for the linear model

$$\Delta\dot{h} = \tilde{A}\Delta h + \tilde{B}\Delta u + d_p,$$

with d_p some noise signal. In summary, the developed results were capable of designing a structured controller in the standard feedback loop from multiple finite-horizon dissipativity specifications purely on the basis of plant data, which achieves good tracking and disturbance attenuation.

5. Conclusion and outlook

5.1. Summary

This thesis introduced a data-driven controller design method for SISO systems based on L-dissipativity conditions for the closed loop in the standard feedback loop. In Chapter 3, the existing results for open-loop systems were extended to the closed loop. More precisely, a parametrization of all closed-loop trajectories, based on one open-loop input-output measurement of the plant and a model of the controller, for all input-output channels has been developed. The key ingredient for developing this trajectory representation was the commutativity property of SISO systems. This parametrization was then used for closed-loop simulation and more importantly to perform a dissipativity analysis on the feedback loop in form of a sufficient and necessary definiteness condition on one single matrix. Since the developed trajectory parmetrization is linear in the controller parameter, the definiteness conditions for disspativity were turned into a QMIFP in Chapter 4 for controller synthesis. A solution for the resulting synthesis inequality can be obtained either through LMI techniques directly, when the present QMI is convex, or through the DC programming approach in the general case. In summary, the present thesis provides a purely data-driven controller design method, allowing to perform multiobjective structured controller design and hence provides a controller synthesis framework in the field of data-driven control.

5.2. Future work

Altough this work provides a promising framework for data-driven controller design, it can and has to be extended to be more applicable on real world problems. Mainly, there are three further directions for future research.

1. MIMO: The provided design framework only deals with SISO plants, because of their commutativity property, and an interesting issue for future research is the extension to general MIMO LTI sytems.

2. Noise: In this thesis, only deterministic LTI systems are considered. More explicitly, the developed guarantees hold only for noise-free measurements, which is in practice usually not the case. Therefore, it is necessary to develop guarantees for this framework when noise is present, which would increase the applicability tremendously.

3. Infinite horizon: The developed results regarding dissipativity, are finite-horizion dissipativity guarantees. To match the well-known dissipativity results from the model-based setting, the existing results have to be extended to the infinite-horizon case. Nonetheless, the finite-horizon case can be useful in practice when choosing the horizon large enough, see Section 4.4.

If further research is conducted on the described points, a purely data-driven controller design framework for general MIMO LTI systems on the basis of infinite-horizon dissipativity specifications would be desirable similar to the model-based setting, which can then be used for controller synthesis in the standard feedback loop for real noisy plants.

A. Appendix

A.1. Auxiliary Lemmas

Lemma A.1 (Adapted from [6]) *Suppose U,$V \in \mathbb{S}$, not necessarily the same size.*

- *Let $U \prec 0$. Then,*
$$V - W^\top U^{-1} W \preccurlyeq 0$$
is equivalent to
$$\begin{pmatrix} U & W \\ W^\top & V \end{pmatrix} \succcurlyeq 0.$$
- *Let $V \prec 0$. Then,*
$$U - W V^{-1} W^\top \preccurlyeq 0$$
is equivalent to
$$\begin{pmatrix} U & W \\ W^\top & V \end{pmatrix} \succcurlyeq 0.$$

These statements hold also when replacing $\prec$ with $\succ$ and $\preccurlyeq$ with $\succcurlyeq$, respectively.

Proof See the proof in [6] for the *Schur Complement* for non-strict inequalities and apply the additional constraints from this Lemma. ■

Lemma A.2 ([13, Corollary 7.1.5]) *Let $A \in \mathbb{S}^n$ be positive semidefinite. Then,* $\operatorname{trace}(A) = 0$ *if and only if* $A = 0$.

Eigenständigkeitserklärung

Ich versichere hiermit, dass ich, Nils Wieler, die vorliegende Arbeit selbstständig angefertigt, keine anderen als die angegebenen Hilfsmittel benutzt und sowohl wörtliche, als auch sinngemäß entlehnte Stellen als solche kenntlich gemacht habe. Die Arbeit hat in gleicher oder ähnlicher Form noch keiner anderen Prüfungsbehörde vorgelegen. Weiterhin bestätige ich, dass das elektronische Exemplar mit den anderen Exemplaren übereinstimmt.

_____ _____

Ort, Datum Unterschrift

Literaturverzeichnis

[1] MOSEK ApS. *The MOSEK optimization toolbox for MATLAB manual. Version 9.2.*, 2019.

[2] J. Berberich and F. Allgöwer. A trajectory-based framework for data-driven system analysis and control. In *2020 European Control Conference (ECC)*, pages 1365–1370, 2020.

[3] J. Berberich, J. Köhler, M. A. Muller, and F. Allgöwer. Data-driven model predictive control with stability and robustness guarantees. *IEEE Transactions on Automatic Control*, 2020.

[4] J. Berberich, A. Koch, C. W. Scherer, and F. Allgöwer. Robust data-driven state-feedback design. In *2020 American Control Conference (ACC)*, pages 1532–1538, 2020.

[5] C. M. Bishop. *Pattern Recognition and Machine Learning*. Springer-Verlag, 2006.

[6] S. Boyd, L. El Ghaoui, E. Feron, and V. Balakrishnan. *Linear Matrix Inequalities in System and Control Theory*, volume 15 of *Studies in Applied Mathematics*. SIAM, Philadelphia, 1994.

[7] D. A. Bristow, M. Tharayil, and A. G. Alleyne. A survey of iterative learning control. *IEEE Control Systems Magazine*, 26(3):96–114, 2006.

[8] M.C. Campi, A. Lecchini, and S.M. Savaresi. Virtual reference feedback tuning: a direct method for the design of feedback controllers. *Automatica*, 38(8):1337 – 1346, 2002.

[9] J. Coulson, J. Lygeros, and F. Dörfler. Data-enabled predictive control: In the shallows of the DeePC. In *2019 European Control Conference (ECC)*, pages 307–312, 2019.

[10] M. Dahleh, M. A. Dahleh, and G. Verghese. Lectures on dynamic systems and control. 2004.

[11] C. De Persis and P. Tesi. Formulas for data-driven control: Stabilization, optimality, and robustness. *IEEE Transactions on Automatic Control*, 65:909–924, 2020.

[12] D. Hill and P. Moylan. Dissipative dynamical systems: Basic input-output and state properties. *Journal of the Franklin Institute*, 309:327–357, 1980.

[13] R.A. Horn and C.R. Johnson. *Matrix Analysis*. Cambridge University Press, 2nd edition, 2013.

[14] Z.-S. Hou and Z. Wang. From model-based control to data-driven control: Survey, classification and perspective. *Information Sciences*, 235:3 – 35, 2013.

[15] IDC and Statista. Volume of data/information created, captured, copied, and consumed worldwide from 2010 to 2024 (in zettabytes).

[16] A. Koch, J. Berberich, J. Köhler, and F. Allgöwer. Determining optimal input-output properties: A data-driven approach. *arXiv preprint arXiv:2002.03882*, 2020.

[17] H. Kwakernaak. Mixed sensitivity design. In *IFAC Proceedings Volumes*, volume 35, pages 61–66, 2016.

[18] H.A. Le Thi and T. Pham Dinh. DC programming and DCA: Thirty years of developments. *Mathematical Programming*, 169:5–68, 2018.

[19] J. Löfberg. YALMIP : A toolbox for modeling and optimization in MATLAB. In *Proceedings of the CACSD Conference*, Taipei, Taiwan, 2004.

[20] L. Ljung. *System Identification: Theory for The User*. Prentice Hall, 1987.

[21] I. Markovsky. Closed-loop data-driven simulation. *International Journal of Control*, 83, 2010.

[22] I. Markovsky and P. Rapisarda. On the linear quadratic data-driven control. In *2007 European Control Conference (ECC)*, pages 5313–5318, 2007.

[23] I. Markovsky and P. Rapisarda. Data-driven simulation and control. *International Journal of Control*, 81:1946–1959, 2008.

[24] T.M. Maupong, J.C. Mayo-Maldonado, and P. Rapisarda. On Lyapunov functions and data-driven dissipativity. *IFAC-PapersOnLine*, 50(1):7783 – 7788, 2017.

[25] T.M. Maupong and P. Rapisarda. Data-driven control: A behavioral approach. *Systems & Control Letters*, 101:37 – 43, 2017.

[26] Y.S. Niu and T. Pham Dinh. DC programming approaches for BMI and QMI feasibility problems. *Advances in Intelligent Systems and Computing*, 282:37–63, 2014.

[27] M. Norrlöf and S. Gunnarsson. Time and frequency domain convergence properties in iterative learning control. *International Journal of Control*, 75(14):1114–1126, 2002.

[28] T. Pham Dinh and H.A. Le Thi. Convex analysis approach to D.C. programming: Theory, algorithm and applications. *Acta Mathematica Vietnamica*, 22(1):289–355, 1997.

[29] A. Romer, J. Berberich, J. Köhler, and F. Allgöwer. One-shot verification of dissipativity properties from input–output data. *IEEE Control Systems Letters*, 3(3):709–714, 2019.

[30] C. Scherer, P. Gahinet, and M. Chilali. Multiobjective output-feedback control via LMI optimization. *IEEE Transactions on Automatic Control*, 42, 1997.

[31] C. Scherer and S. Wieland. Linear matrix inequalities in control. *Lecture Notes, Dutch Institute for Systems and Control, Delft*, 2015.

[32] H. D. Tuan, P. Apkarian, S. Hosoe, and H. Tuy. D.C. optimization approach to robust control: Feasibility problems. *International Journal of Control*, 73(2):89–104, 2000.

[33] H. J. van Waarde, C. De Persis, M. K. Camlibel, and P. Tesi. Willems' fundamental lemma for state-space systems and its extension to multiple datasets. *IEEE Control Systems Letters*, 4:602–607, 2020.

[34] Y. Wang and R. Rajamani. Feasibility analysis of the bilinear matrix inequalities with an application to multi-objective nonlinear observer design. In *2016 IEEE 55th Conference on Decision and Control (CDC)*, pages 3252–3257, 2016.

[35] N. Wieler, J. Berberich, A. Koch, and F. Allgöwer. Data-driven controller design via finite-horizon dissipativity. In *Proceedings of the 3rd Conference on Learning for Dynamics and Control*. PMLR, 2021. To appear, preprint online: arXiv:2101.06156.

[36] J. C. Willems. Dissipative dynamical systems. Part I: General theory. *Arch. Rational Mech. Anal.*, 45:321–350, 1972.

[37] J. C. Willems. Dissipative dynamical systems. Part II: Linear systems with quadratic supply rates. *Arch. Rational Mech. Anal.*, 45:352–392, 1972.

[38] J. C. Willems, P. Rapisarda, I. Markovsky, and B. De Moor. A note on persistency of excitation. *Systems & Control Letters*, 54:325–329, 2005.